無容器法により合成した超高屈折率ガラスの物性と構造

東京大学生産技術研究所
増野敦信

Collaborators

H. Inoue, K. Yoshimoto, Y. Kikuchi, T. Mizoguchi, Y. Watanabe

Institute of Industrial Science, The University of Tokyo

J, Yu, Y. Arai, M. Kaneko

Japan Aerospace Exploration Agency (JAXA)

S. Kohara

Japan Synchrotron Radiation Research Institute

Y. Kuroiwa, C. Moriyoshi

Hiroshima University

K. Okajima

Saga-LS

A. C. Hannon

ISIS Facility, Rutherford Appleton Laboratory

E. Bychkov

Université du Littoral

Introduction

Containerless processing

with container	without container
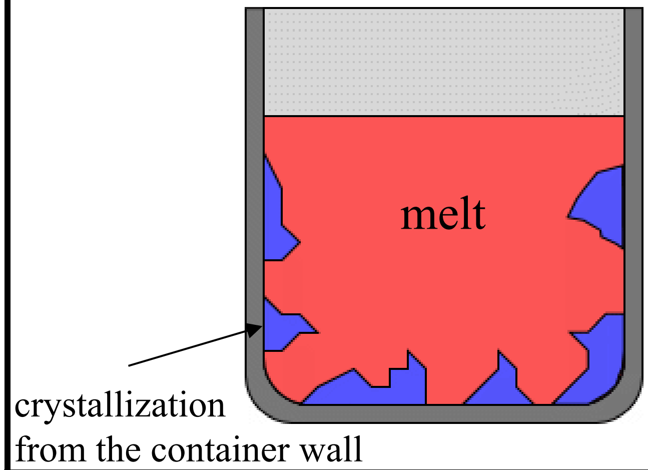	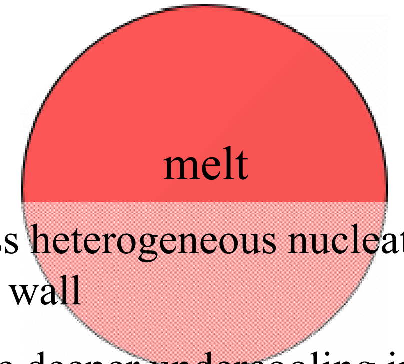 ✓suppress heterogeneous nucleation from the container wall ✓promote deeper undercooling in molten materials
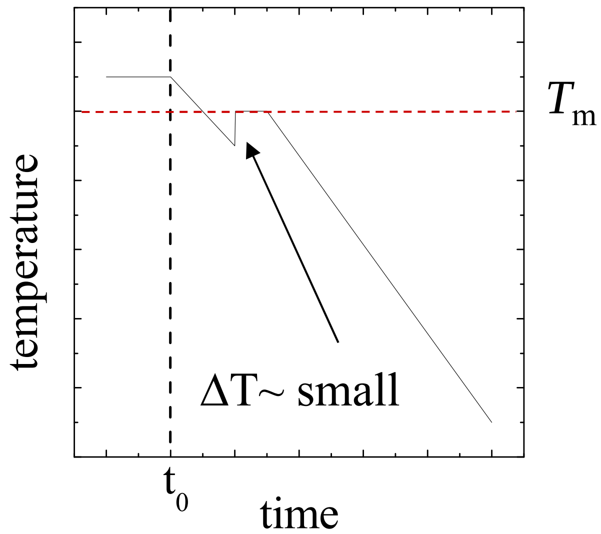	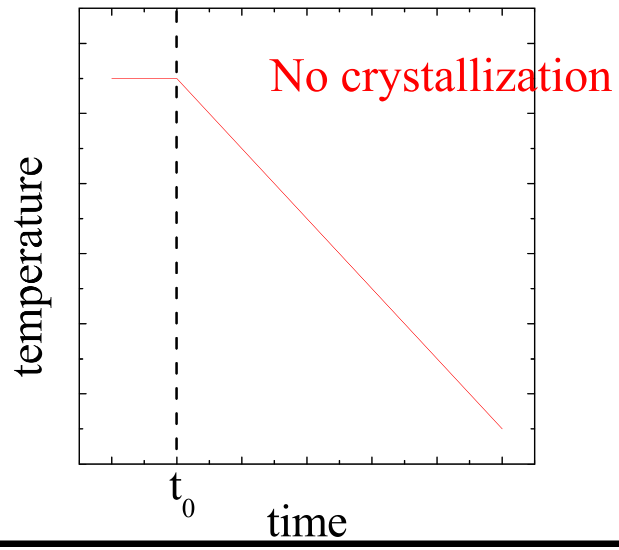

Containerless processing on the ground

Various types of levitation furnace

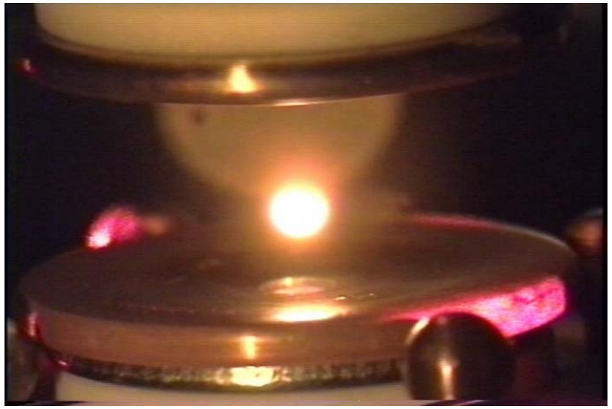

Electrostatic levitation furnace

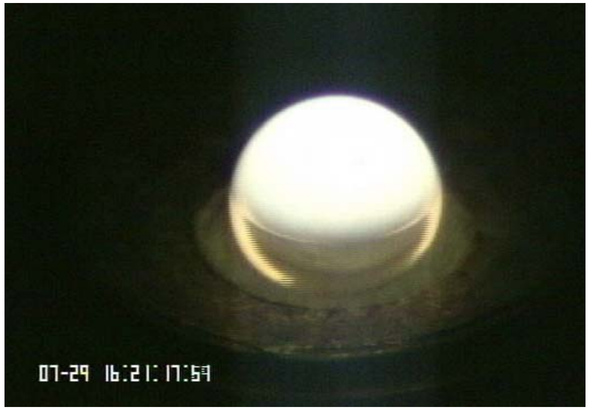

Aerodynamic levitation furnace

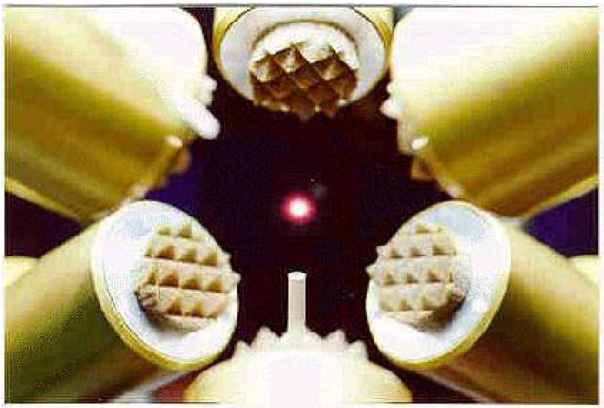

Acoustic wave levitation furnace

Electromagnetic levitation furnace

Aerodynamic levitation furnace

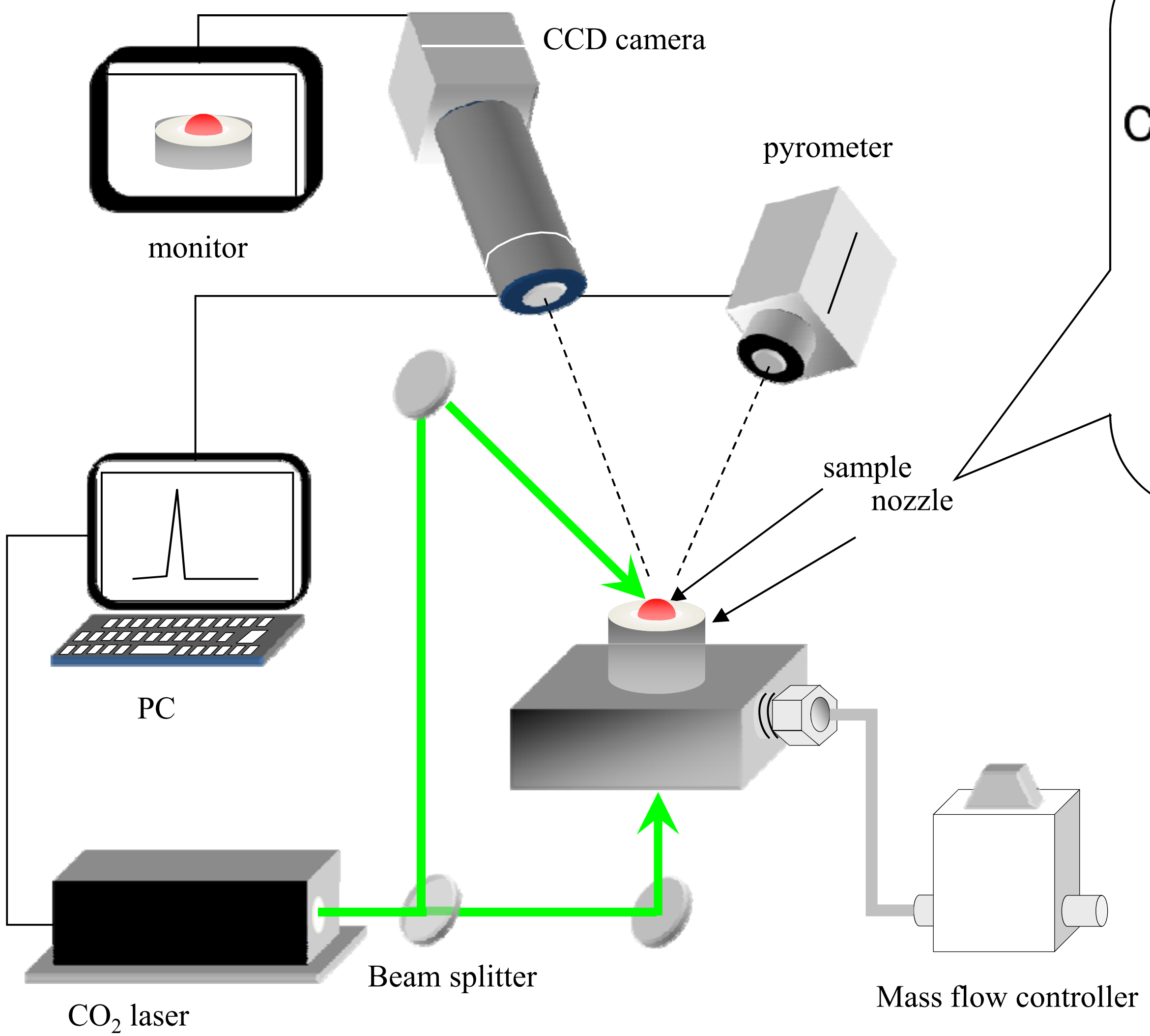

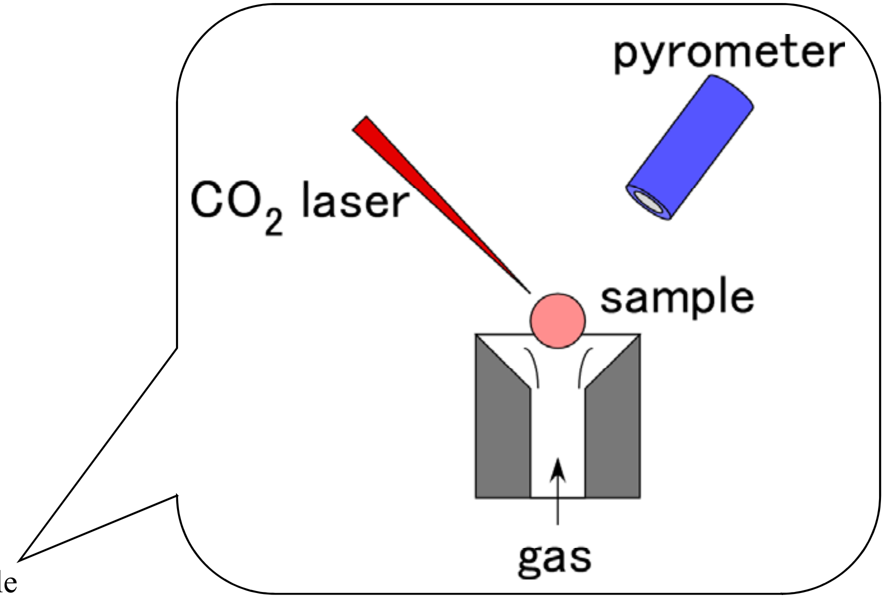

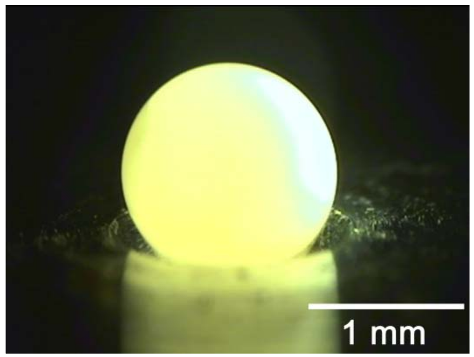

Gas: air, oxygen, nitrogen, argon
Pressure: 1 ~ 3 atm
Sample size: ϕ = 1 ~ 5 mm
Sample weight: 10 ~ 200 mg

Ferroelectric $BaTi_2O_5$

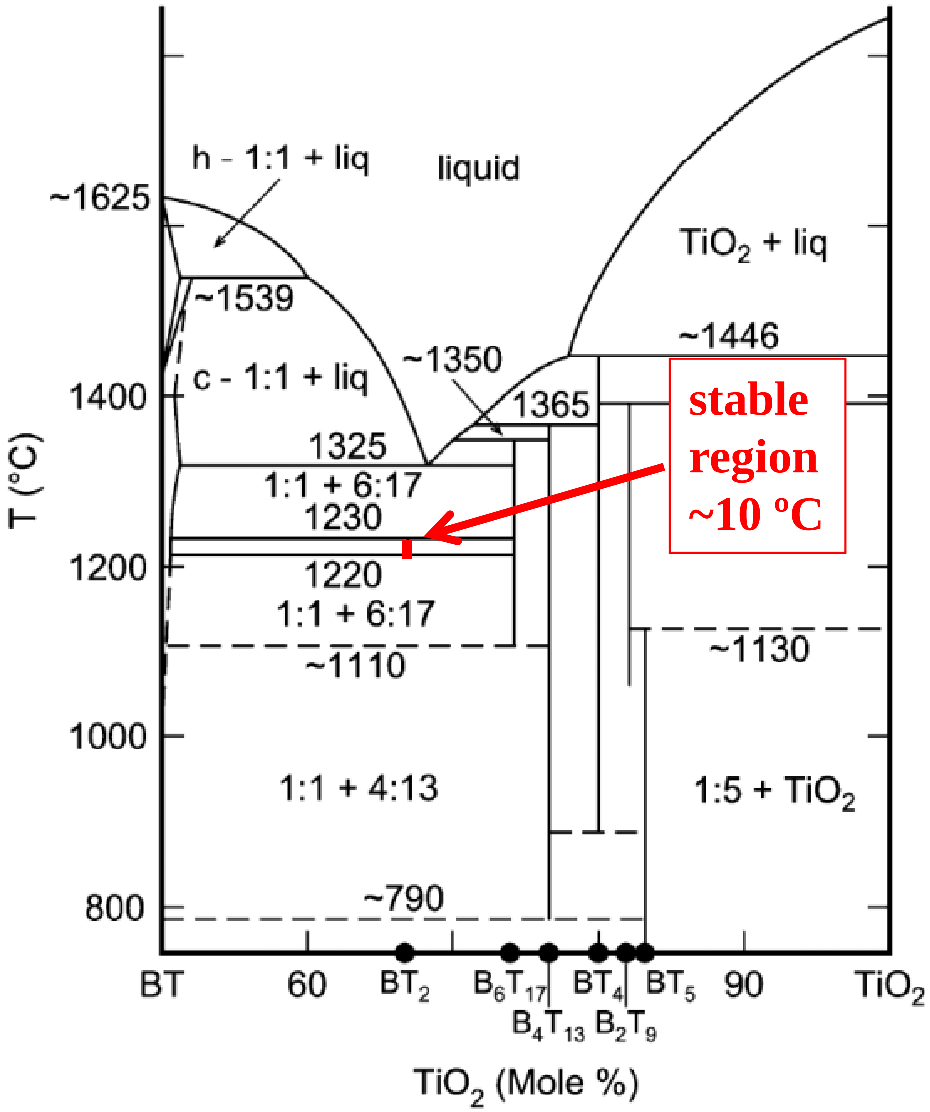

N. Zhu and A. R. West, J. Am. Ceram. Soc. **93**, (2010) 295.

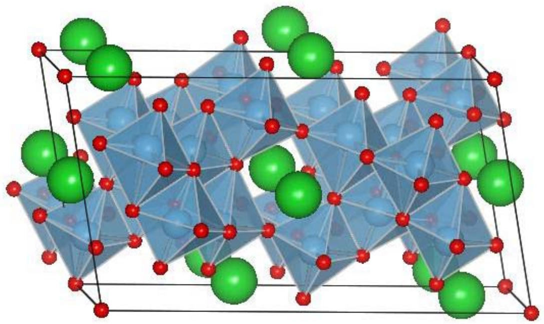

Monoclinic,
a = 1.6914 nm,
b = 0.3935 nm,
c = 0.9412 nm
b = 103.11º

Y. Akishige *et al*., Jpn. J. Appl. Phys. **42**, (2003) L946.
T. Akashi, *et al*., Mater. Trans. **44**, (2003) 1644.

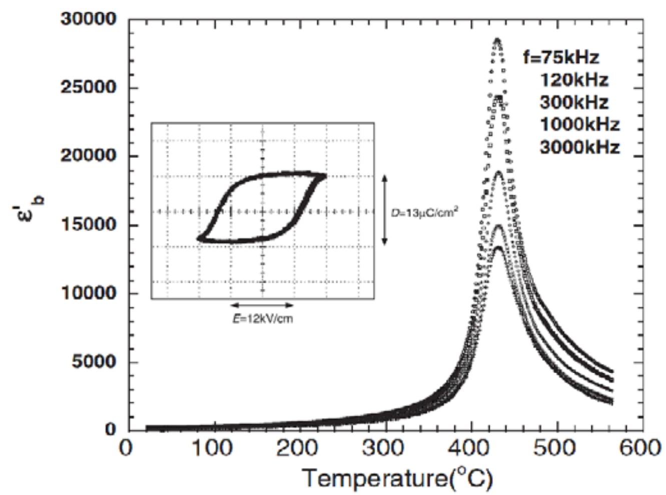

✓High ferroelectric transition temperature
✓Large dielectric constant
✓Colorless and transparent

Glass formation of ferroelectric $BaTi_2O_5$

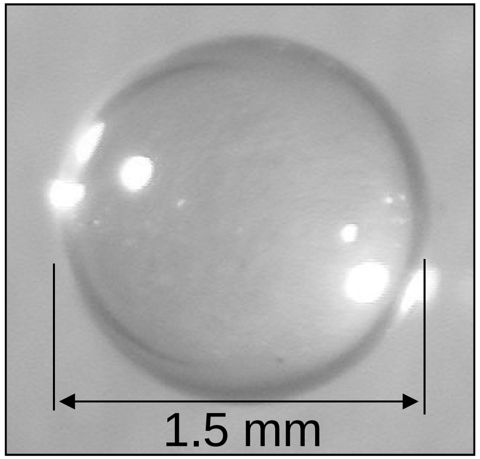

J.Yu *et al*., Chem. Mater. **18**, (2006) 2169.

The first time glass formation of ferroelectric titanate without any network former oxides.

✓Glass structure
- Distorted TiO_5 polyhedra
- Edge shared polyhedra

✓Crystallization process
- Metastable phase formation
- Giant dielectric response

XRD, ND

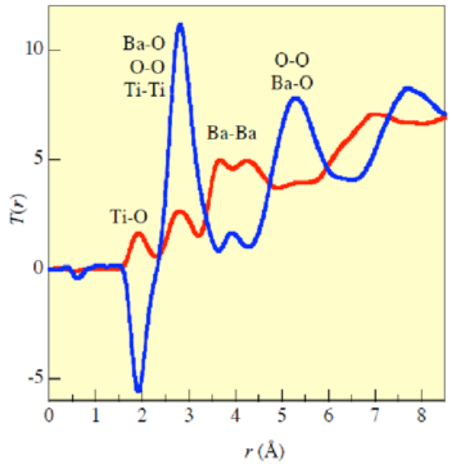

XANES

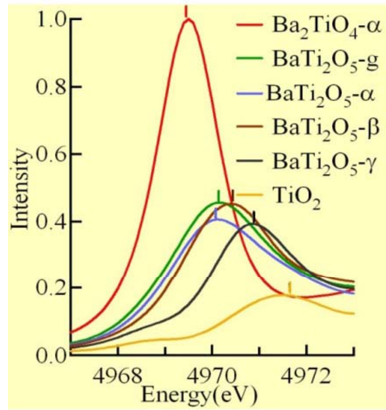

RMC simulation

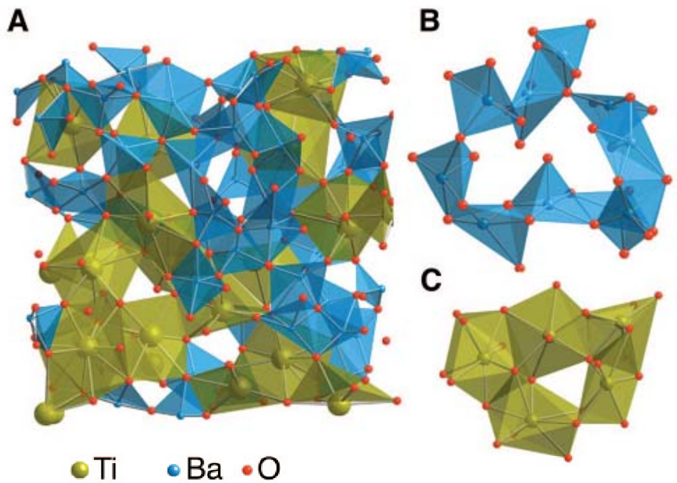

J.Yu *et al*., Chem. Mater. **21**, (2009) 259.

Metastable phase formation from $BaTi_2O_5$ glass

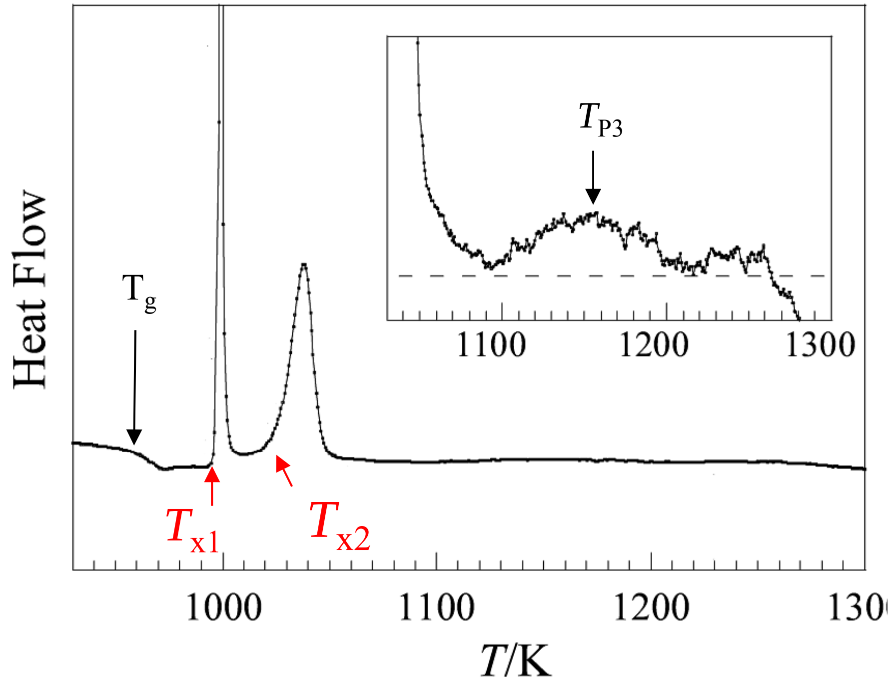

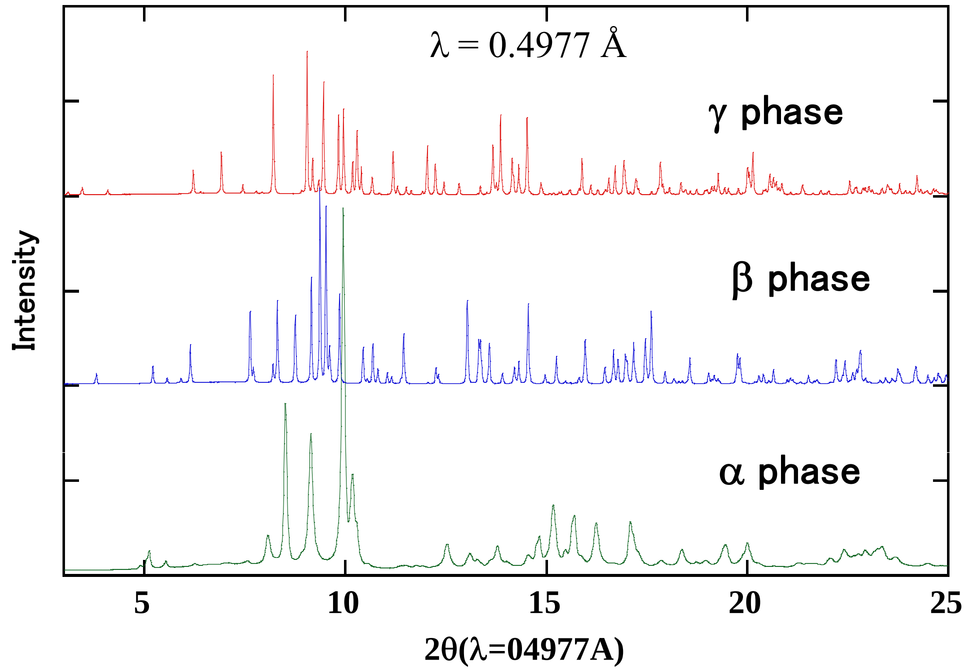

Before crystallization at 1150 K of the stable ferroelectric γ phase, two metastable phases α (at T_{x1}) and β (at T_{x2}) appeared in sequence.

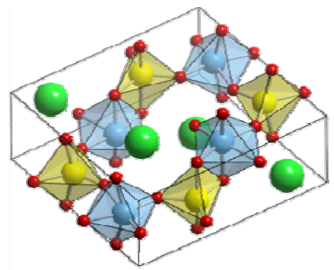

Paraelectric β phase

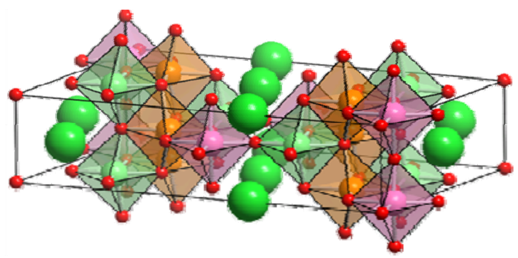

Ferroelectric γ phase

J.Yu *et al.*, Chem. Mater. **21**, (2009) 259.

Giant dielectric response at T_{x1}

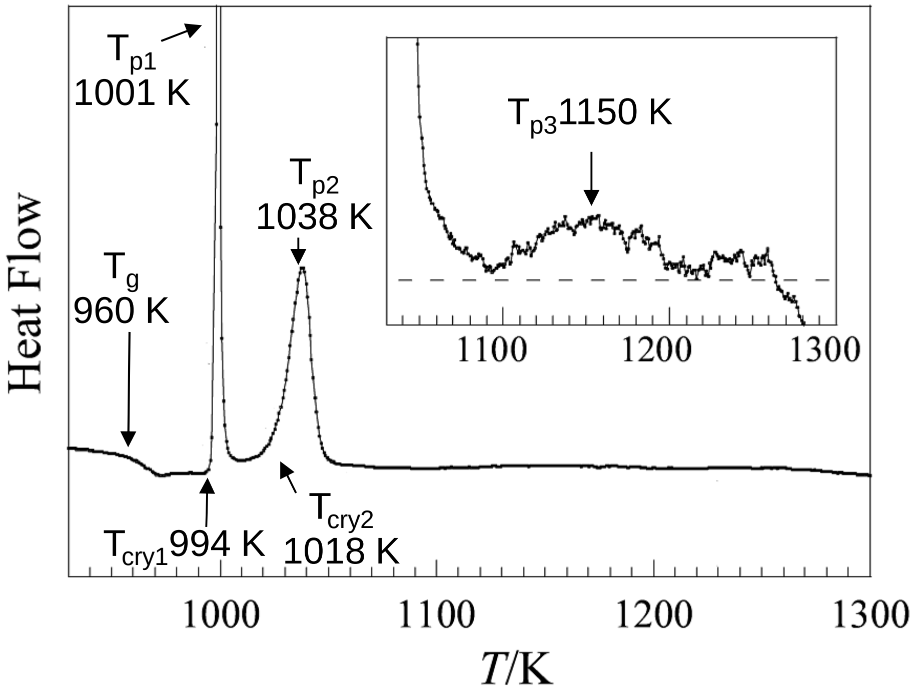

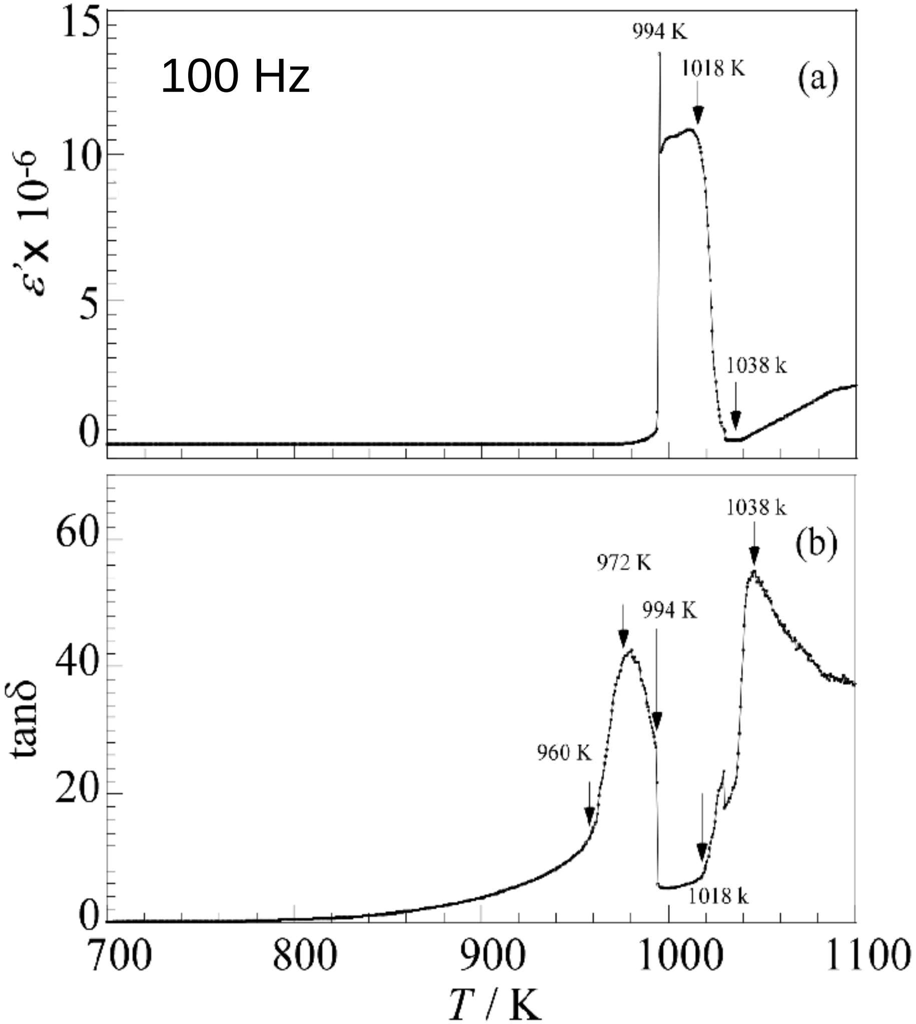

J.Yu *et al*., Chem. Mater. **18**, (2006) 2169.

Next step

✓Optical properties

Transmission

Refractive index

Luminescence properties

✓Glass forming region

binary (La_2O_3-TiO_2)

ternary (BaO-TiO_2-MO_x, La_2O_3-TiO_2-MO_x)

✓Unusual crystallization process

Optical properties

Optical properties of $BaTi_2O_5$ glass

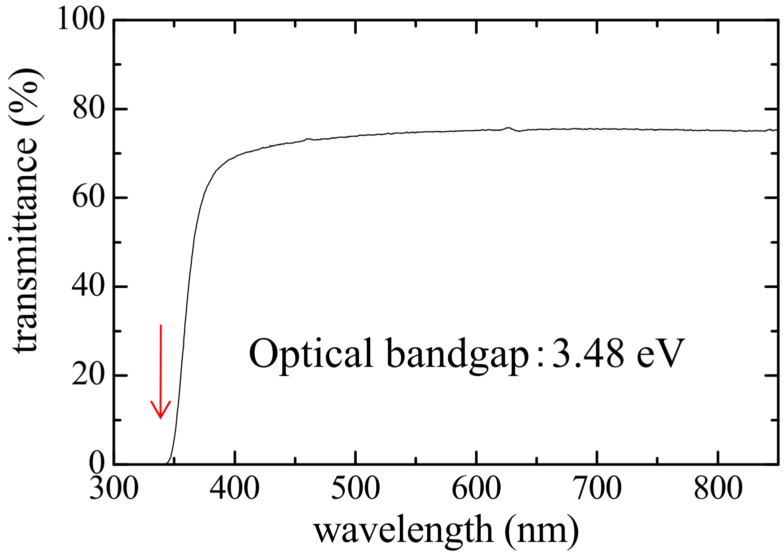

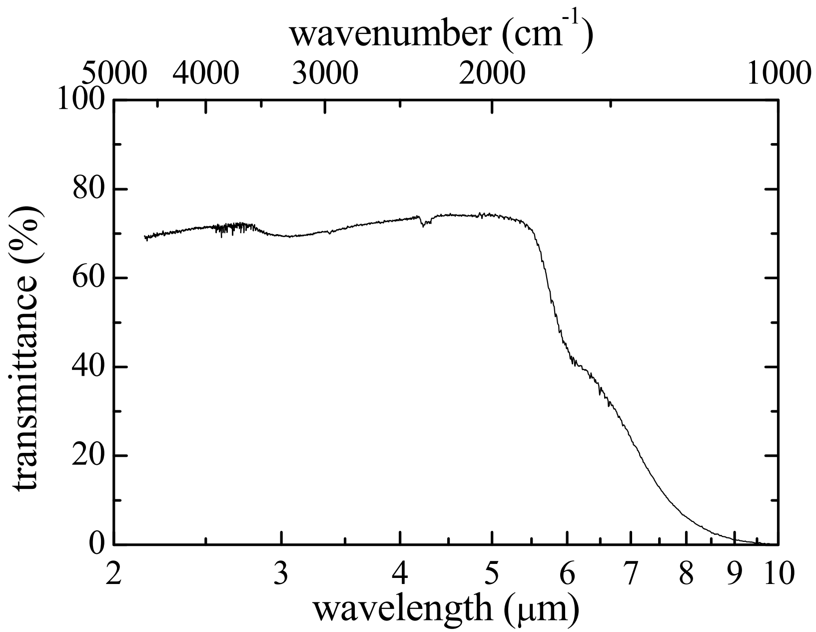

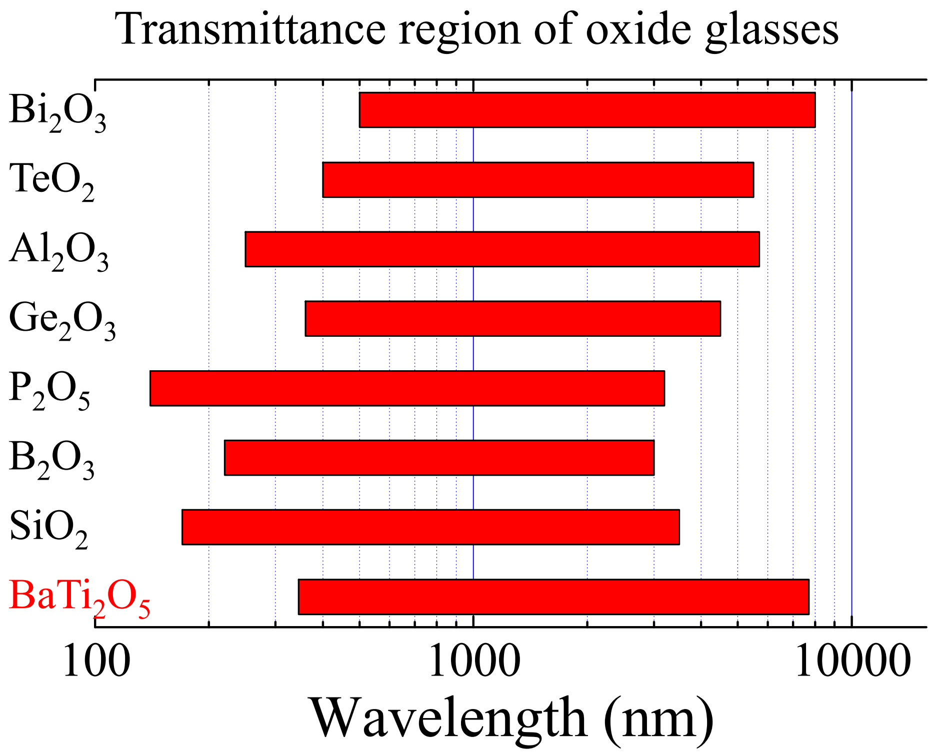

$BaTi_2O_5$ glass: transparent from 350 nm to 7.7 μm

A. Masuno *et al*., J. Appl. Phys. **108**, (2010) 063520.

Refractive index of $BaTi_2O_5$ glass

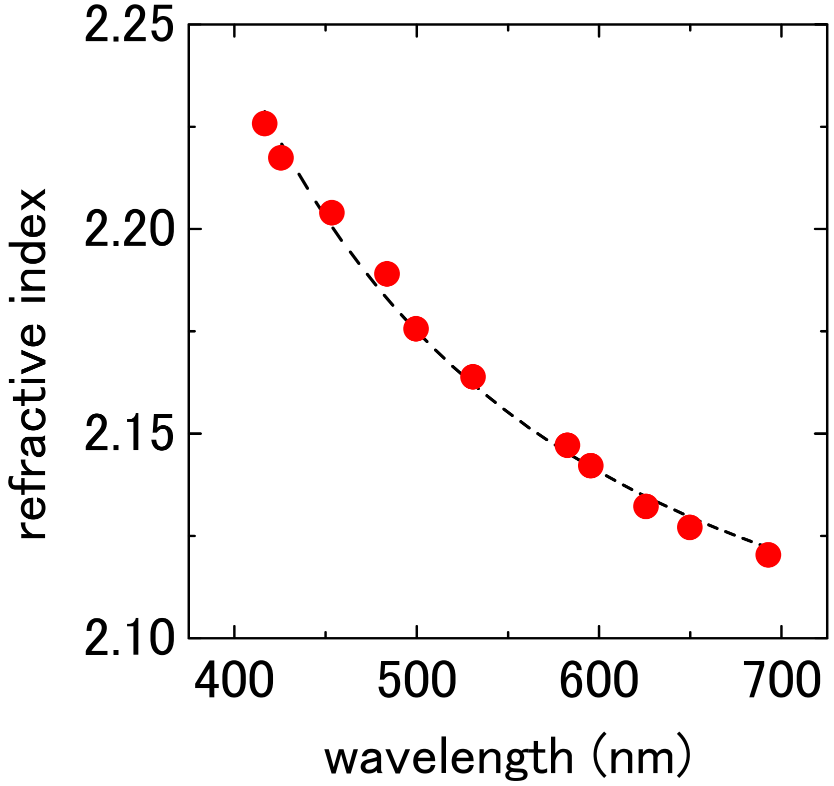

Abbe number $\nu = \dfrac{n_d - 1}{n_F - n_c} = 20.5$

n_F : H F (487 nm)
n_d : He d (587.6 nm)
n_c : H c (656.3 nm)

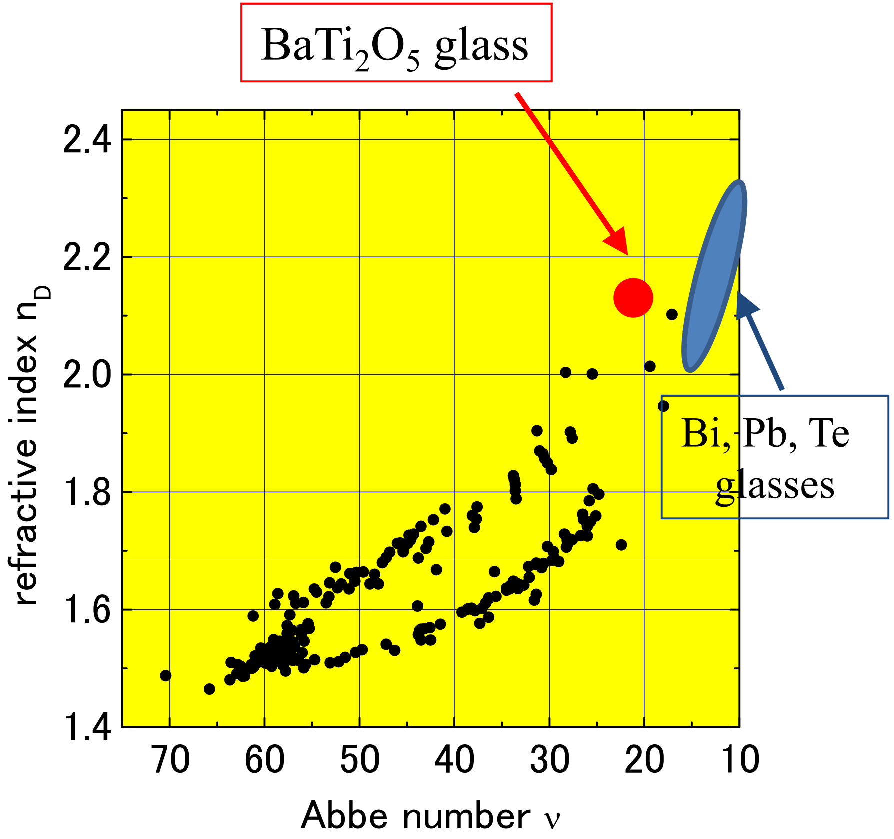

✓Conventional high refractive index glasses contain Bi, Pb, Te.
✓Larger Abbe number of $BaTi_2O_5$ glass among high refractive index glasses

A. Masuno *et al.*, J. Appl. Phys. **108**, (2010) 063520.

Large oxygen polarizability

✓Lorentz-Lorenz equation

$$\frac{(n^2-1)}{(n^2+2)} = \frac{4\pi\alpha_m N_A}{3V_m}$$

N_A: Avogadro's number
α_m: molar polarizability
V_m: molar volume

$V_m = 22.8\ cm^3/mol$

Silicate:30 ~ 60 cm_3/mol
Borate: 25 ~ 45 cm^3/mol
Phosphate: 27 ~ 60 cm^3/mol

✓Oxygen polarizability

$$\alpha_{O^{2-}} = \left(\alpha_m - \sum \alpha_i\right)\left(N_{O^{2-}}\right)^{-1}$$

N_{O2-}:number of oxygen

$\alpha_{Ba2+} = 1.595$ (Å^3)
$\alpha_{Ti4+} = 0.184$ (Å^3)
∴$\Sigma\alpha i = 0.654$ (Å^3)

	α_{O2-}
$20B_2O_3$-$80SiO_2$	1.434
$20Na_2O$-$80B_2O_3$	1.374
$25ZnO$-$75P_2O_5$	1.502
$BaTi_2O_5$	**2.57**

Quite large α_{O2-}

•High ionicity of oxygen
•Large contribution of electrons around oxygen to the high refractive index.

These features are different from conventional oxide glasses.

A. Masuno *et al.*, J. Appl. Phys. **108**, (2010) 063520.

Origin of high refractive index

Elements in $BaTi_2O_5$ glass are highly ionic.

↓

Weaken covalent bond between cations and oxygen

↓

Larger packing density

↓

Higher refractive index

Functionalization by rare-earth doping

$Ba_{0.7}\mathit{Ln}_{0.3}Ti_2O_{5.15}$

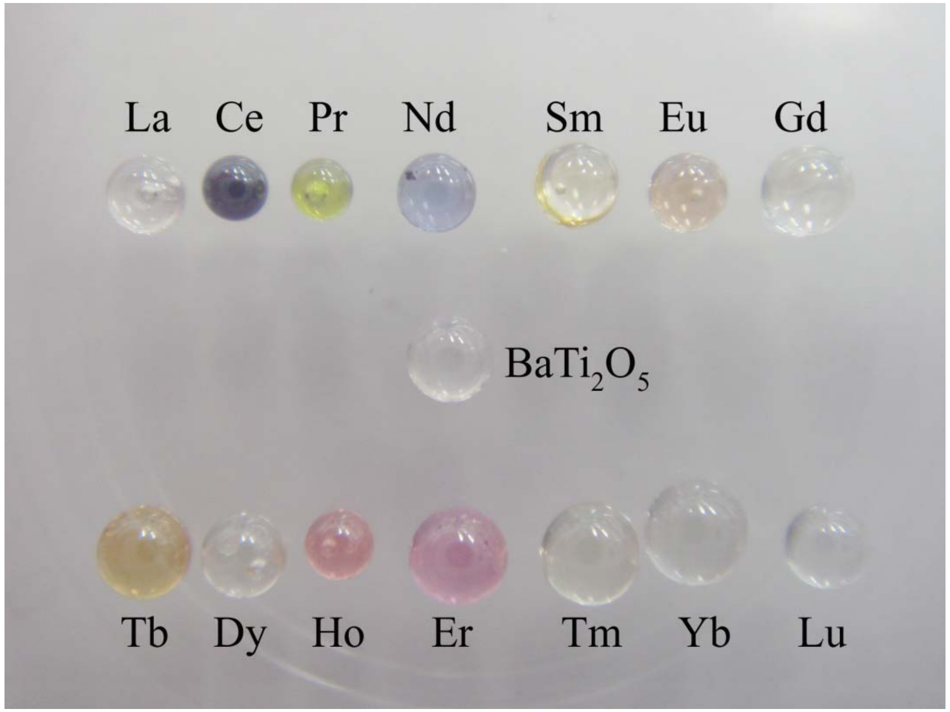

High concentration of *Ln*

Raman scattering

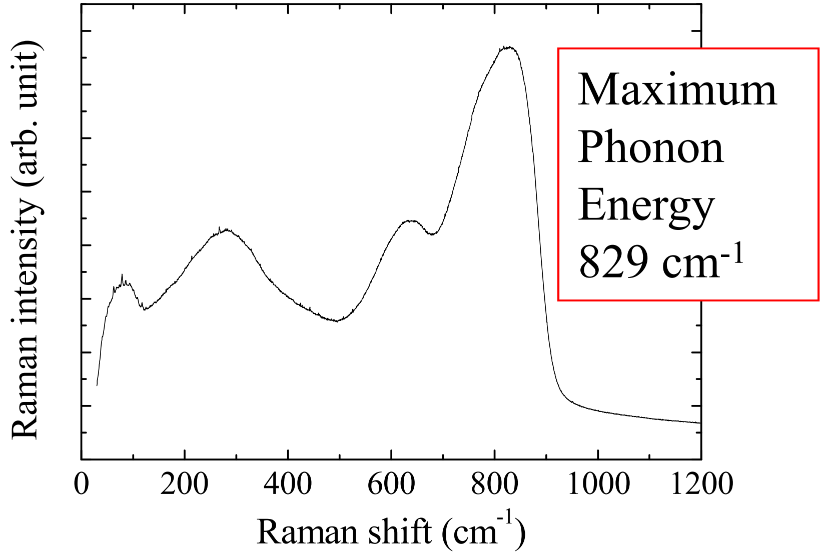

SiO_2 system	1100 cm^{-1}
B_2O_3 system	1265
P_2O_5 system	1360
GeO_2 system	880
TeO_2 system	800
$BaTi_2O_5$	829

Upconversion of Er^{3+} doped $BaTi_2O_5$ glass

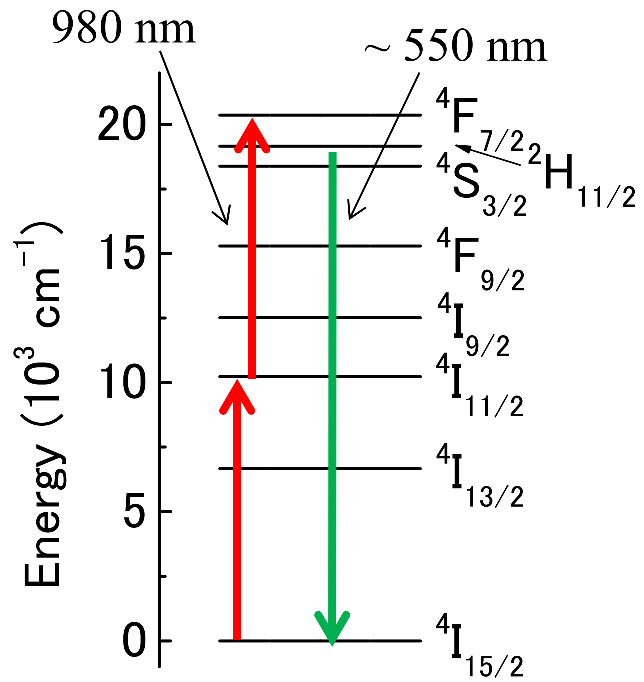

Energy diagram of Er^{3+}

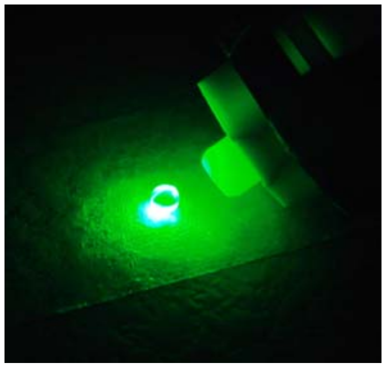

Strong upconversion luminescence

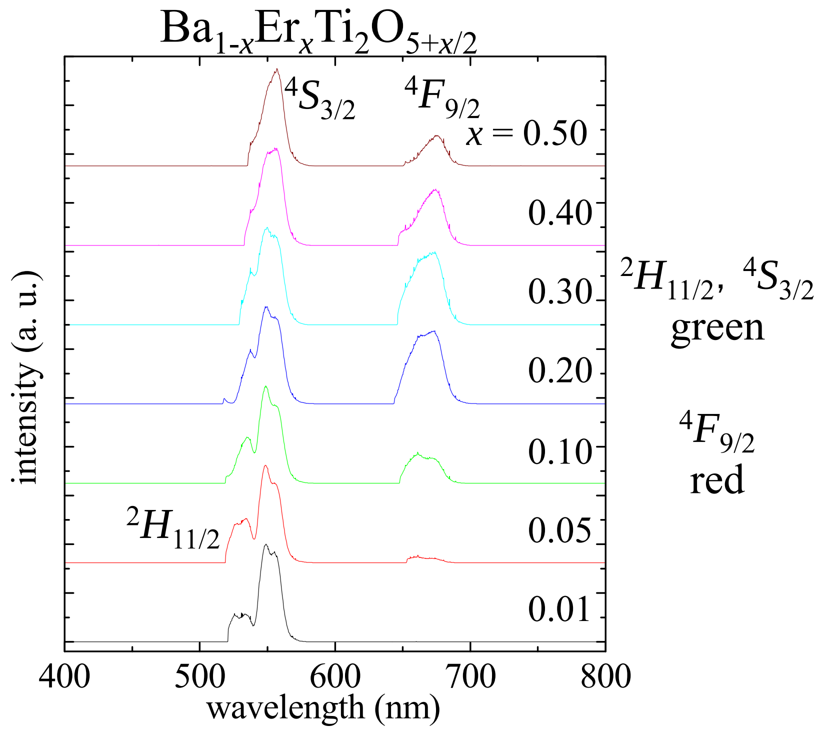

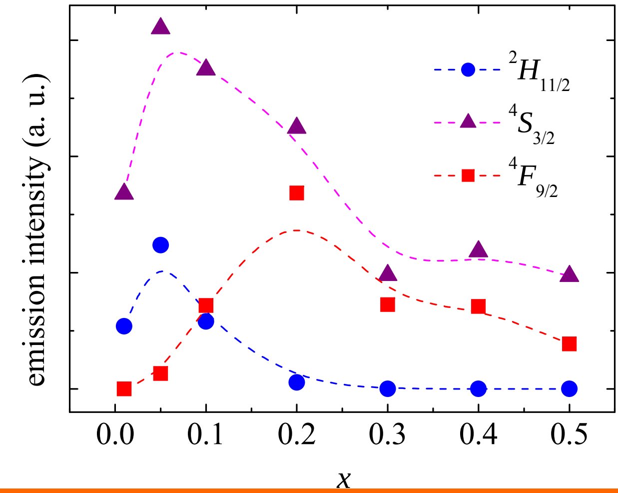

Different composition dependence

Different process

Luminescent process of Er^{3+} doped $BaTi_2O_5$ glass

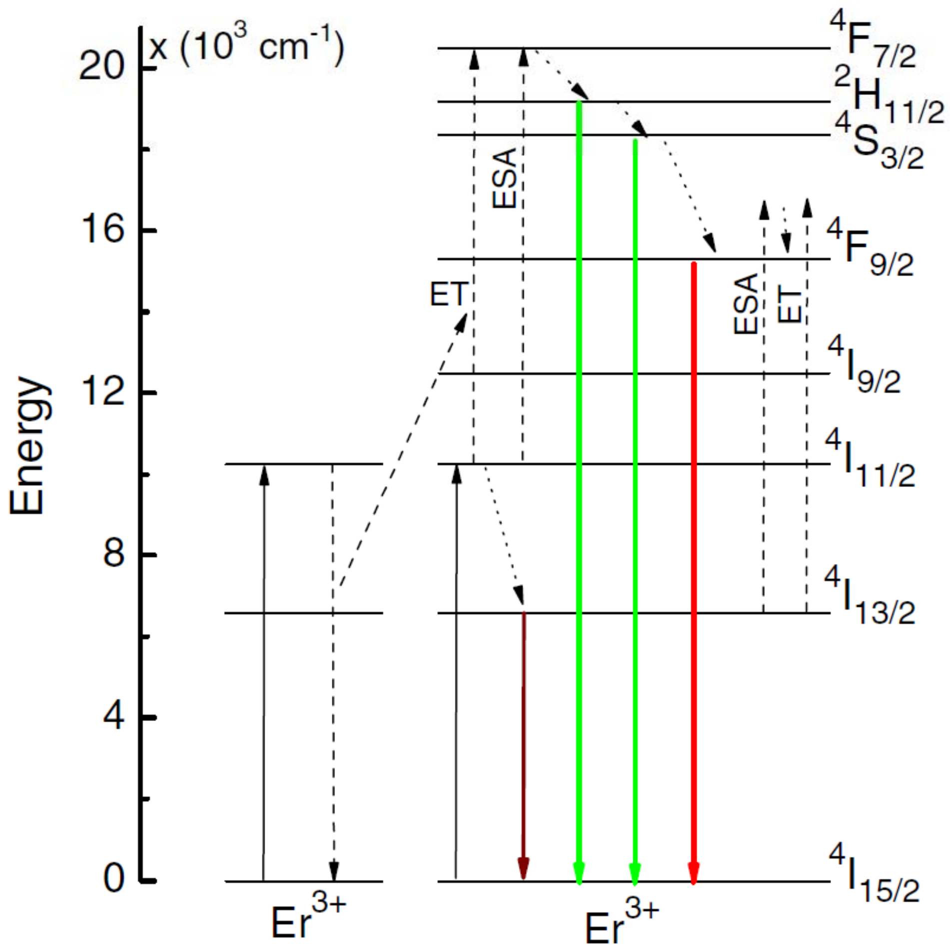

ET: Energy Transfer
ESA: Excited State Absorption

✓Green

ET: $2\ {}^4I_{11/2} \rightarrow {}^4I_{15/2} + {}^4F_{7/2}$

ESA: ${}^4I_{11/2} + h\nu \rightarrow {}^4F_{7/2}$

and then

${}^4F_{7/2} \rightarrow {}^2H_{11/2} \rightarrow {}^4S_{3/2}$

strong luminescence in low concentration

→main process is ESA.

✓Red

Green process + ${}^4S_{3/2} \rightarrow {}^4F_{9/2}$

ET: ${}^4I_{13/2} + {}^4I_{11/2} \rightarrow {}^4I_{15/2} + {}^4F_{9/2}$

ESA: ${}^4I_{13/2} + h\nu \rightarrow {}^4F_{9/2}$

strong luminescence in high concentration

→main: ${}^4S_{3/2} \rightarrow {}^4F_{9/2}$ and ET

Glass forming region

Glass forming region of $Ba_{1-x}A_xTi_2O_5$

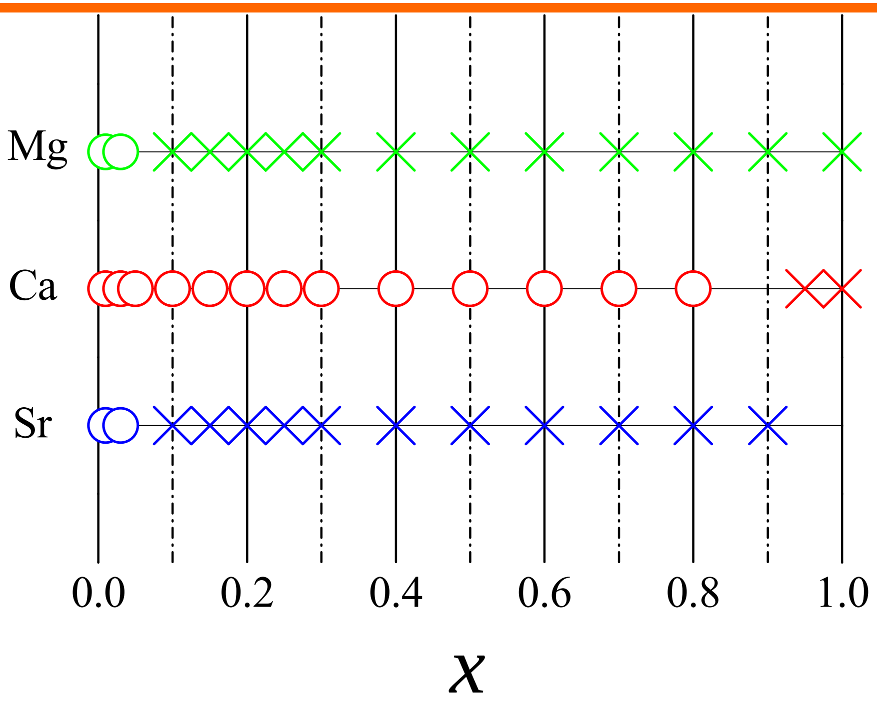

A = Mg, Sr: $x \leq 0.05$

A = Ca: $x \leq 0.90$

Exceptionally large glass-forming region of $Ba_{1-x}Ca_xTi_2O_5$.

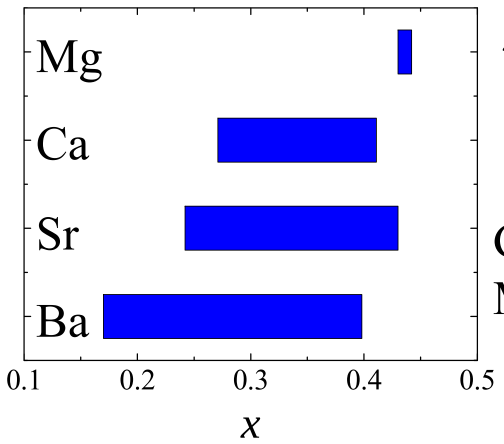

$xAO-(1-x)B_2O_3$

Glass forming region:
Mg < Ca < Sr < Ba

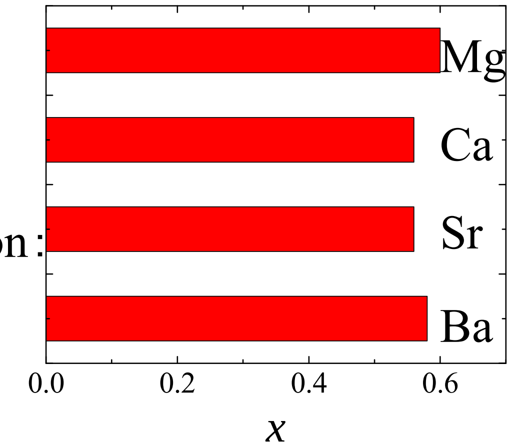

$xAO-(1-x)P_2O_5$

Almost the same regardless of the alkali-earth ion substituted

O. V. Mazurin, M. V. Streltsina, T. P. Shvaiko-Shvaikovskaya (Eds.), Handbook of Glass Data, Physical Science Data 15, Part B (single-component and binary non-silicate oxide glasses), Elsevier, Amsterdam, 1985.

Thermal properties of $Ba_{1-x}Ca_xTi_2O_5$ glasses

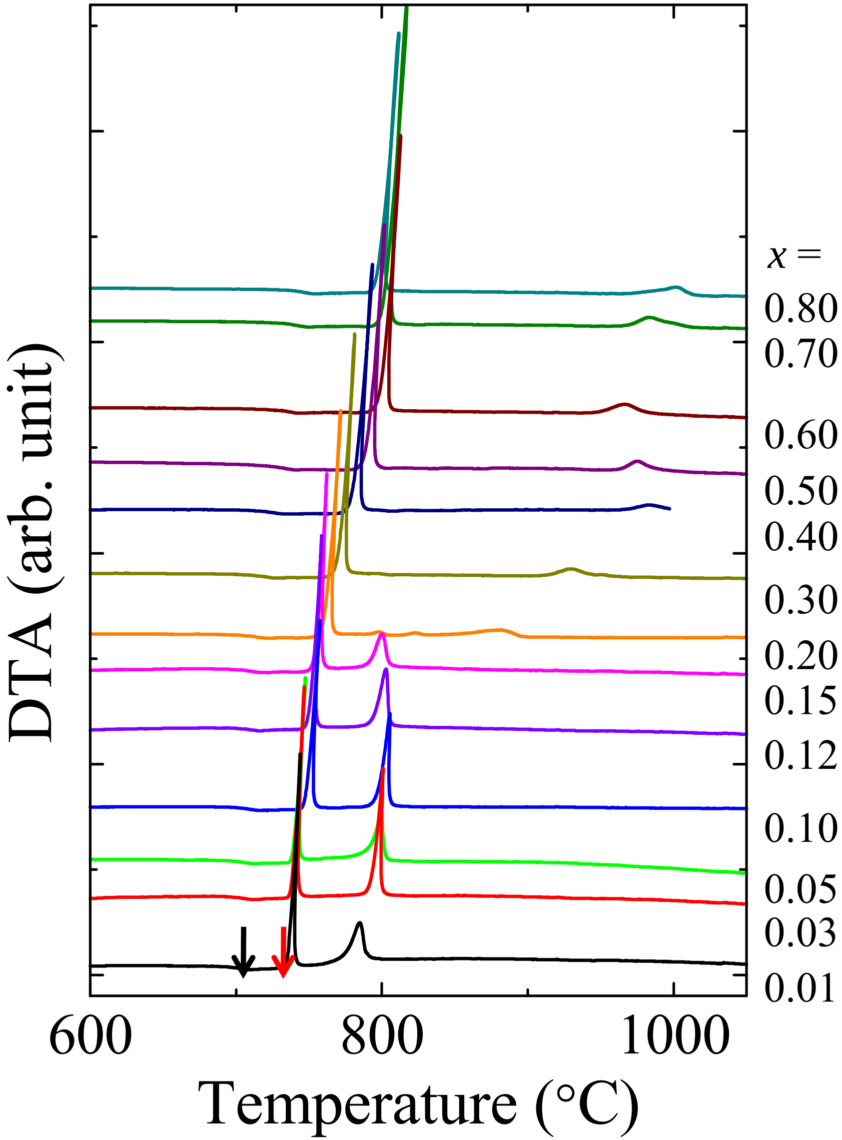

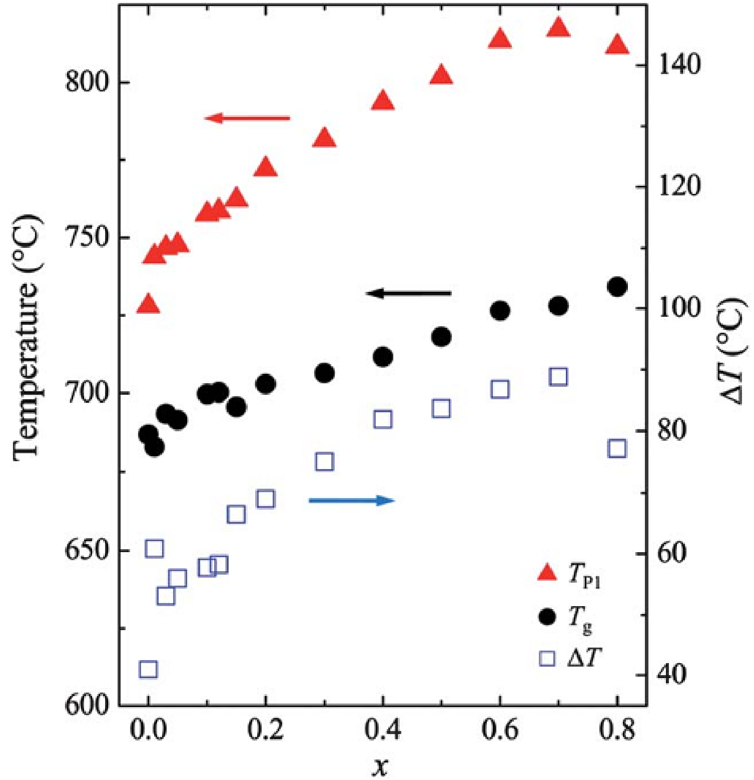

T_g and T_{x1} increased with x.
$\Delta T = T_{x1} - T_g$ increased with x.

A. Masuno *et al.*, J. Mater. Chem. **21**, 17441 (2011).

Refractive index of $Ba_{1-x}Ca_xTi_2O_5$ glasses

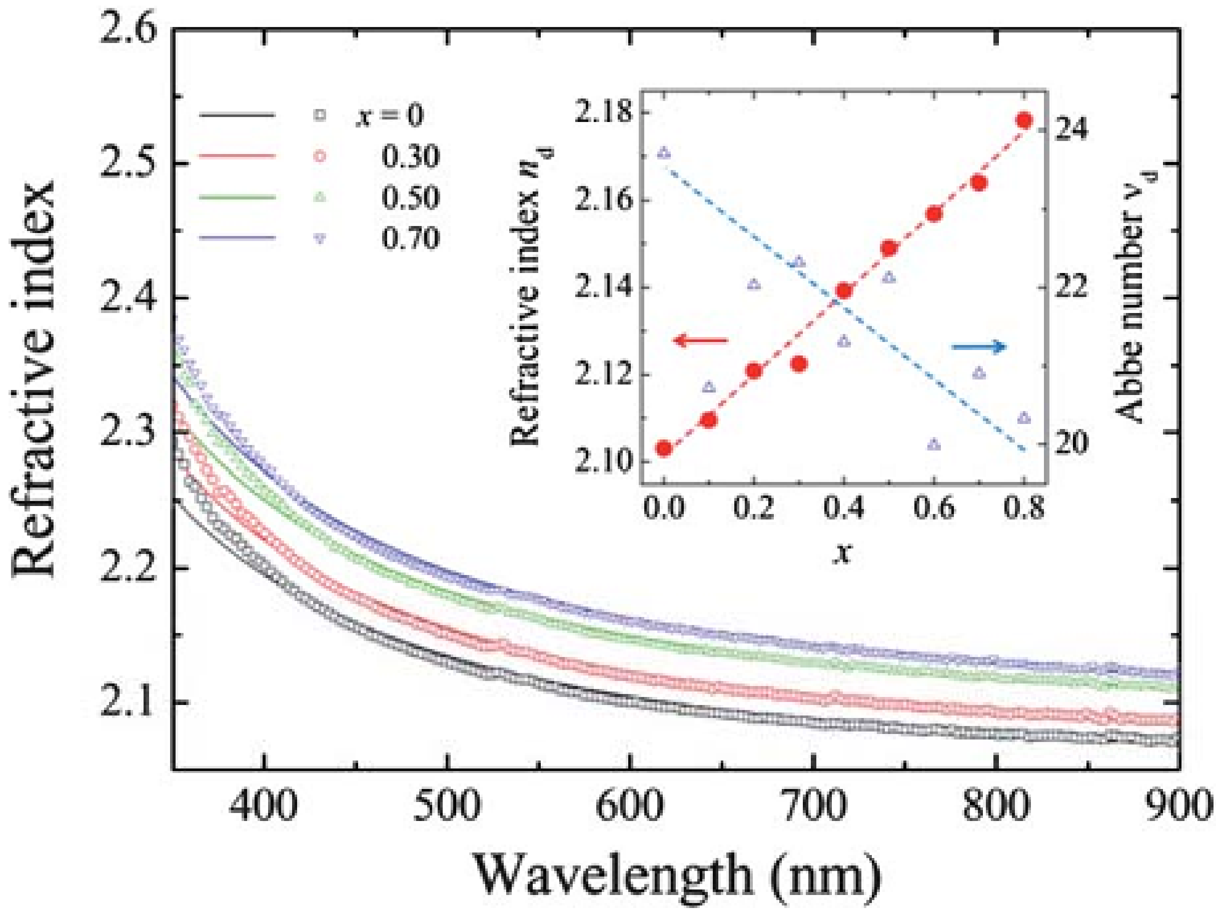

$$\nu_d = \frac{n_d - 1}{n_F - n_C}$$

n_d : 587.6 nm
n_F : 486.1 nm
n_C : 656.3 nm

Refractive index increases with increase of Ca content.
ν_d decreases.

Unexpected result

A. Masuno *et al*., J. Mater. Chem. **21**, 17441 (2011).

Transmittance of $Ba_{1-x}Ca_xTi_2O_5$ glasses

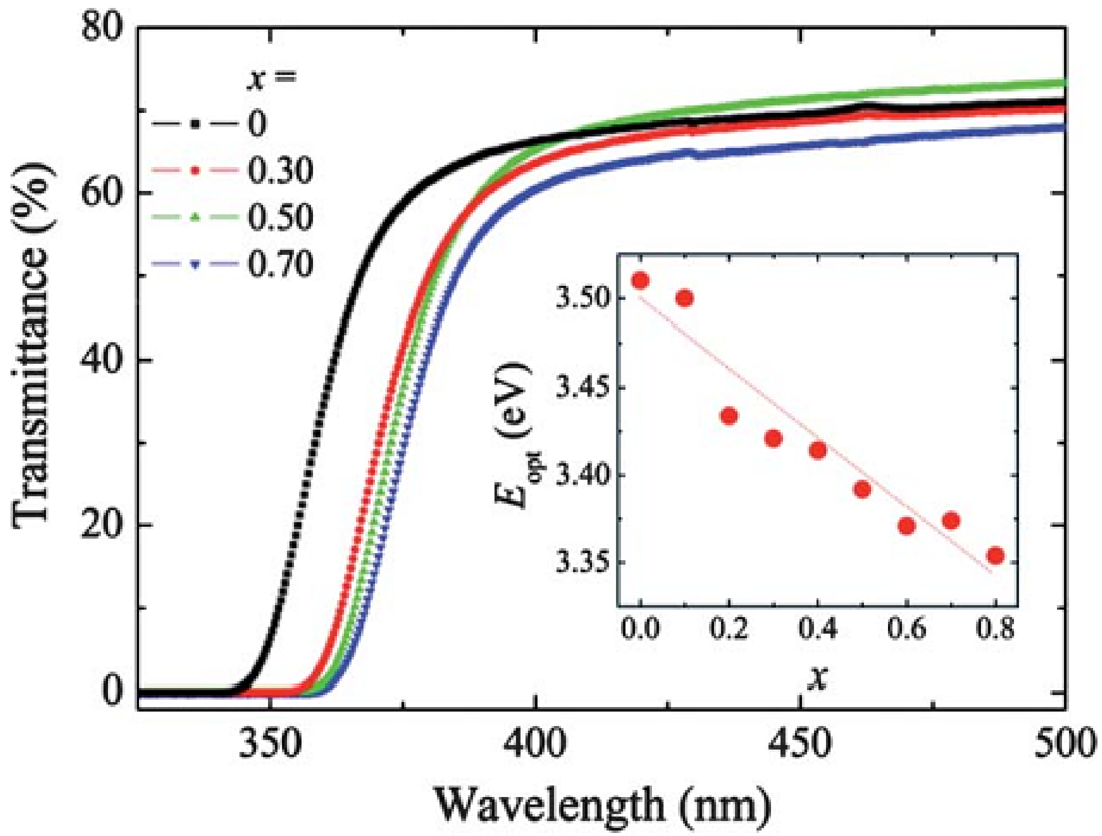

Optical bandgap E_{opt}

$$\alpha h\nu = A\left(h\nu - E_{opt}\right)^2$$

α: the absorption coefficient
h: the Planck constant
ν: the frequency of light
A: an energy-independent constant

E_{opt} decreases with increase of Ca content.

Colorless and transparent
The absorption edge shifted to longer wavelength.

Unexpected result

A. Masuno *et al*., J. Mater. Chem. **21**, 17441 (2011).

Refractive index dispersion and optical bandgap

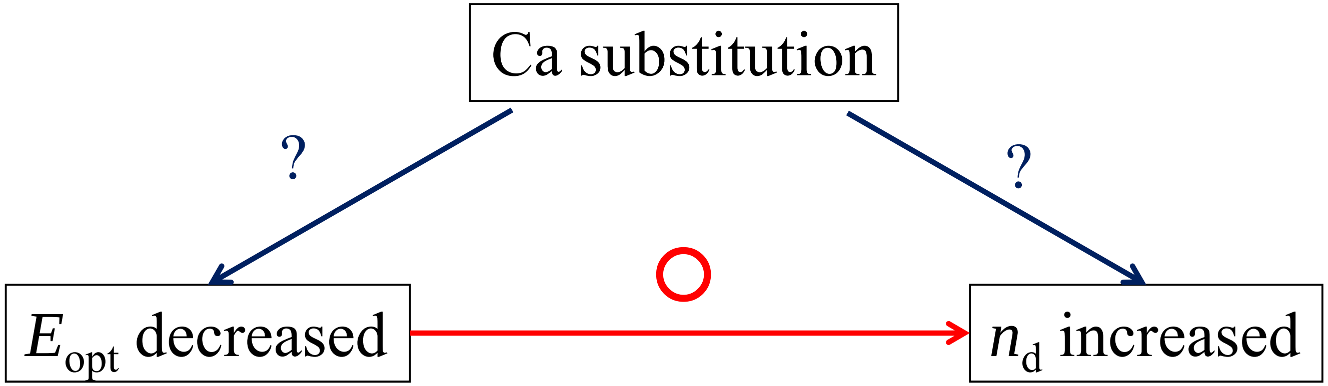

Smaller E_{opt} leads to larger n_d.

The problem:

Why does Ca substitution decrease E_{opt}?

Raman scattering spectra of $Ba_{1-x}Ca_xTi_2O_5$ glasses

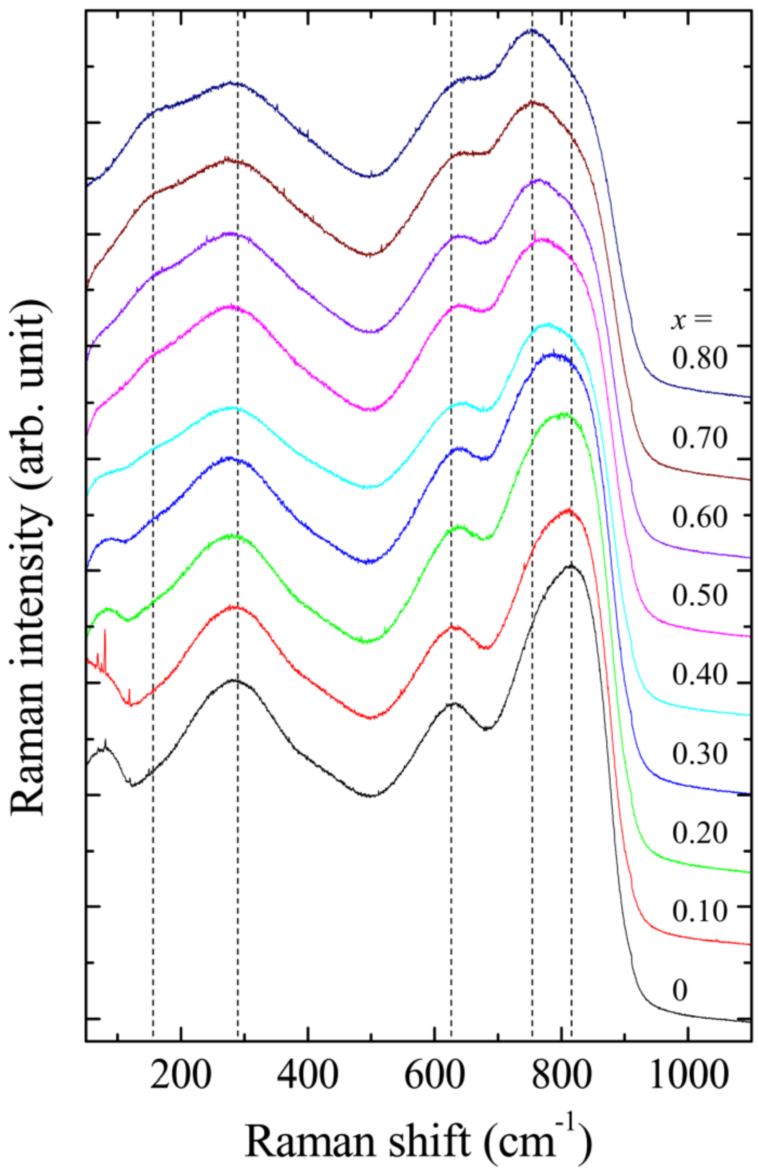

The bands at 636 cm^{-1} and 829 cm^{-1}:
one long Ti–O bond and four short Ti–O bonds

The band at 636 cm^{-1} does not shift.
→one long Ti–O bond remains.

The peak intensity of the band at 829 cm^{-1} decreases and that of the band at 780 cm^{-1} increases.
→the lengths of some of the four short bonds increase
→a narrow distribution of the Ti–O bond length and relaxing the distorted Ti–O polyhedra.

A. Masuno *et al*., J. Mater. Chem. **21**, 17441 (2011).

Bandgap decrease by local structure change

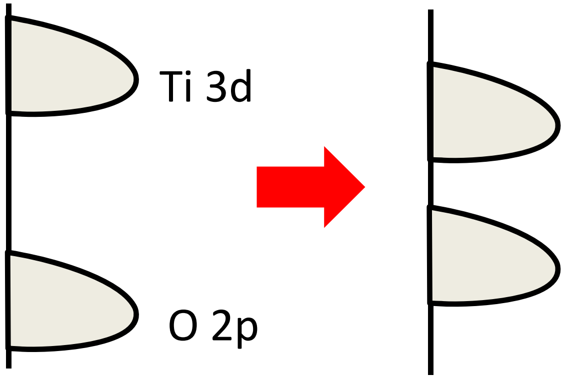

Ti–O bonding state strongly affects the band gap.

a narrow distribution of the Ti–O bond length and relaxing the distortedTi–O polyhedra by lengthening some short Ti-O bonds

→the degree of hybridization of O 2p and Ti 3d orbitals decreases
→the difference between the bond and anti-bond levels becomes smaller
→bandgap decreases
→refractive index increases

Structural-relaxation-induced high refractive index

A. Masuno *et al*., J. Mater. Chem. **21**, 17441 (2011).

The impact of Ca substitution

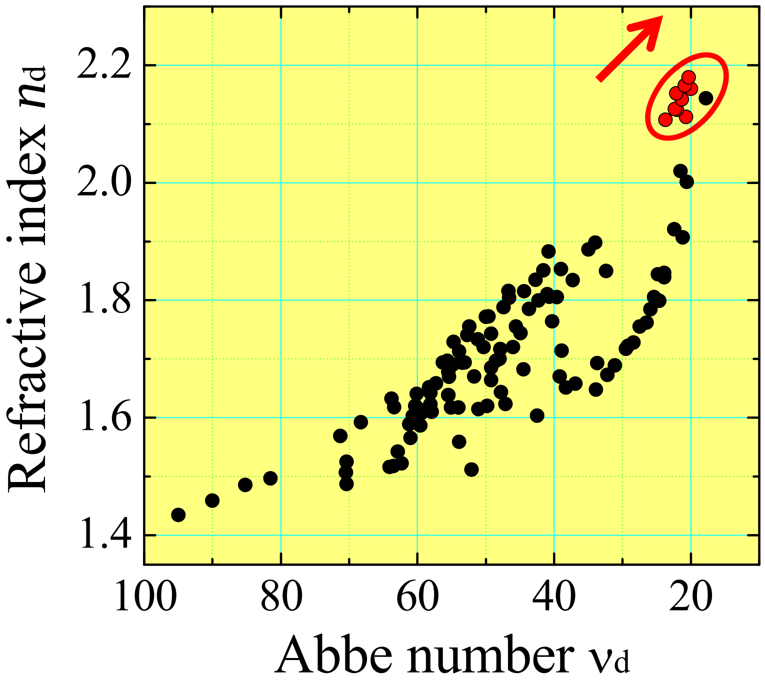

as the Ca^{2+} content increases,…

- Glass are thermally stabilized.
- Optical band gap decreases.
- The refractive index increases.
- The Abbe number decreases.

The changes in the physical properties caused by Ca^{2+} substitution are mainly due to the local structure relaxation caused by their different ionic radii.

Structural-relaxation-induced high refractive index

A. Masuno *et al*., J. Mater. Chem. **21**, 17441 (2011).

Future work for $Ba_{1-x}A_xTi_2O_5$ glasses

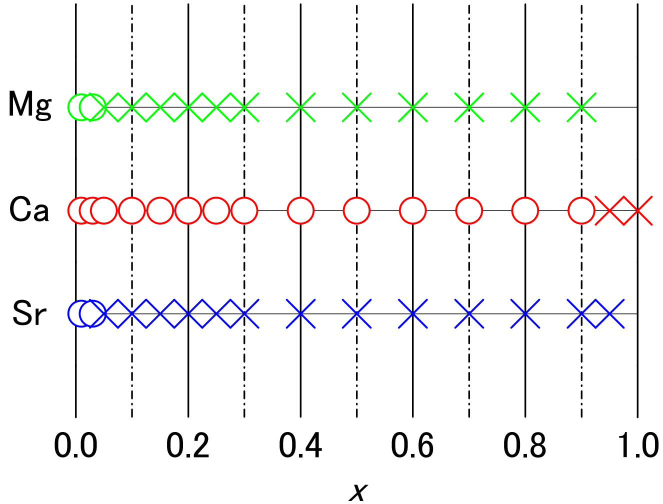

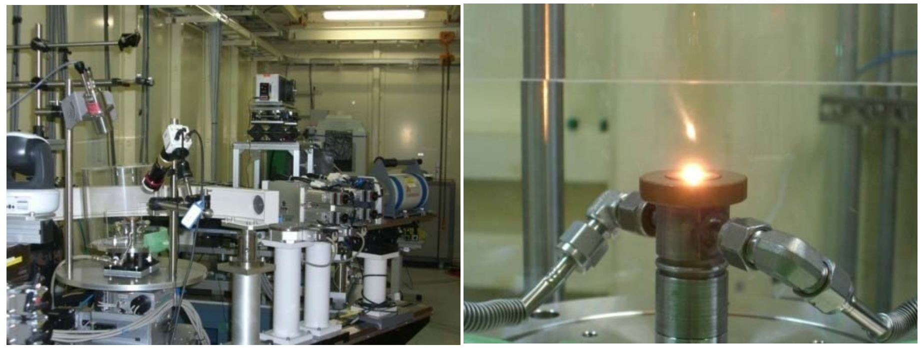

Aerodynamic levitation furnace at SPring-8 BL04B2 for in-situ XRD

Sr is the neighboring element of Ba in the periodic table, and Ca is the second neighbor of Ba. Why glass forming region is narrow in Sr substitution but wide in Ca

Structural analysis of undercooling melt is necessary.

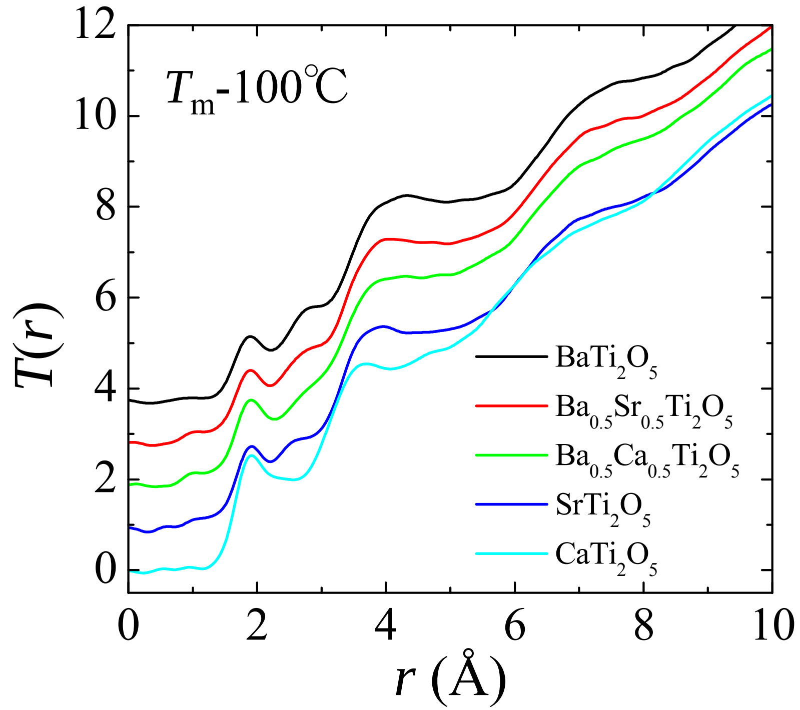

La_2O_3-TiO_2-MO_x system

La_2O_3-TiO_2

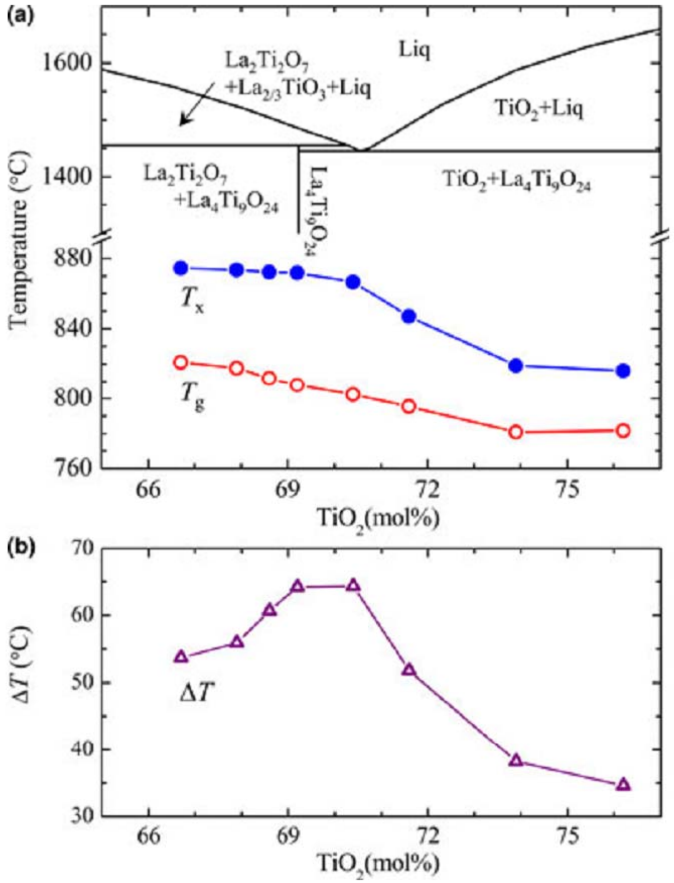

La_2O_3-TiO_2-ZrO_2

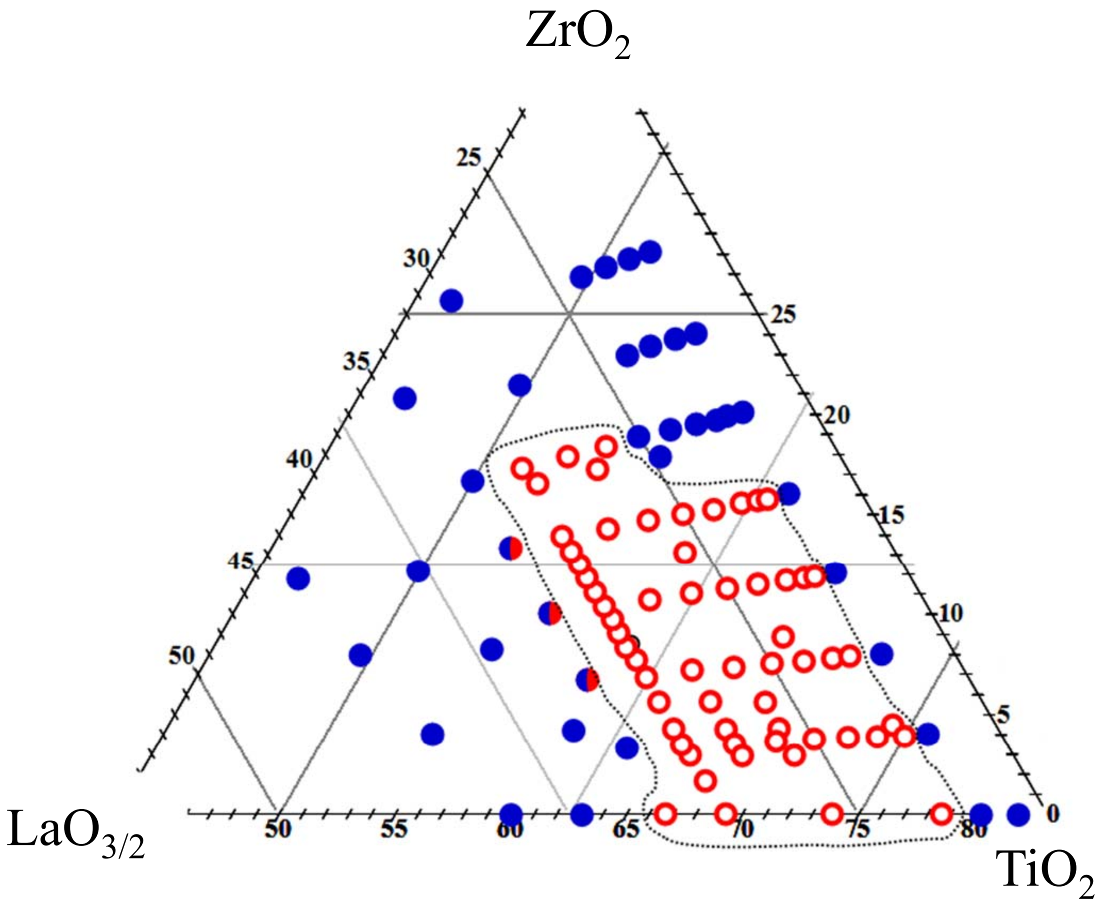

Y. Arai *et al*., J. Appl. Phys. **103**, (2008) 094905.

M. Kaneko *et al*., J. Am. Ceram. Soc. **95**, (2011) 79.

H. Inoue *et al*., Opt. Mater. **33**, (2011) 1853.

Abbe diagram

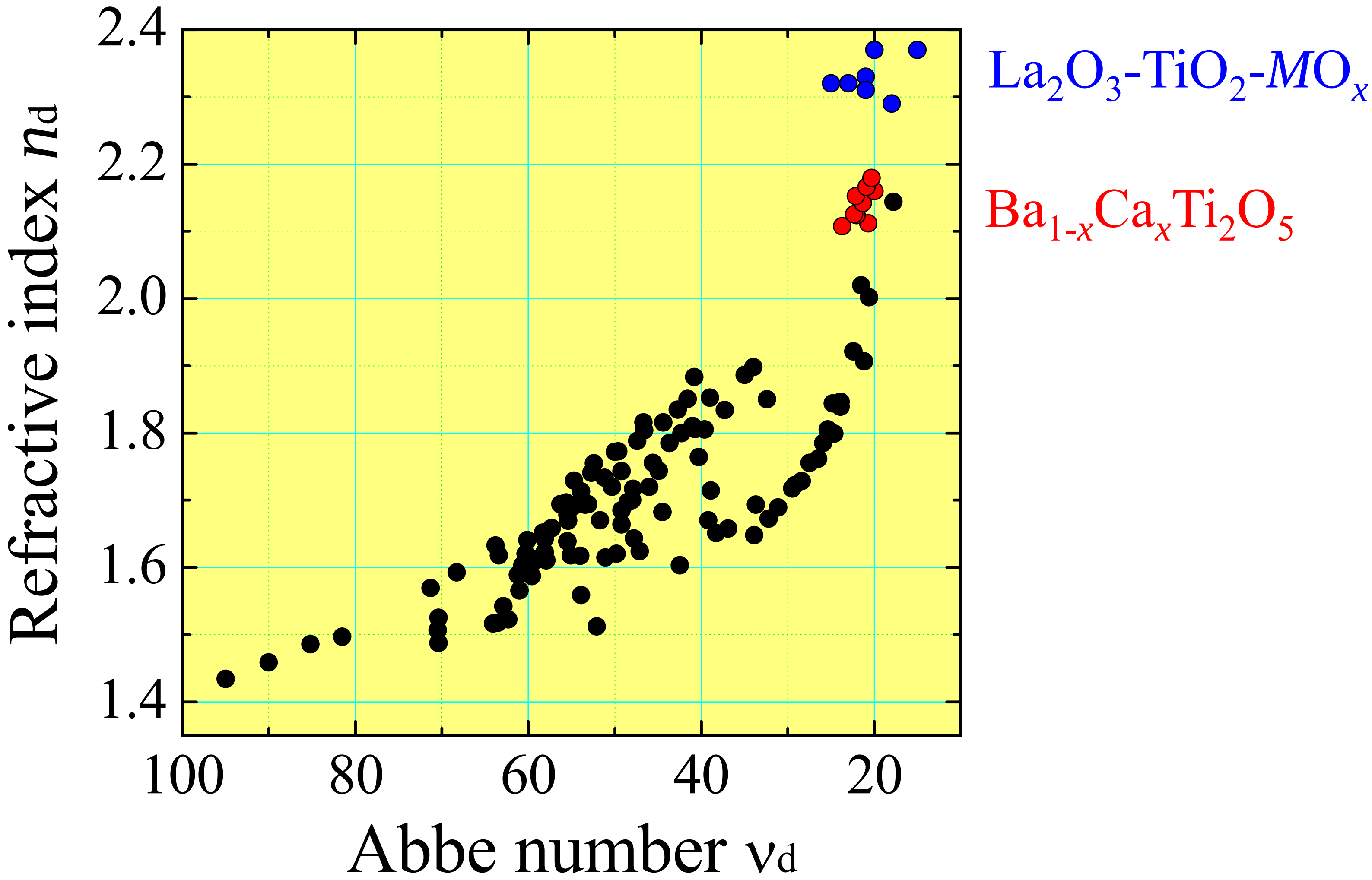

$BaTi_2O_5$ glass

Unusual crystallization process

Metastable phase formation from $BaTi_2O_5$ glass

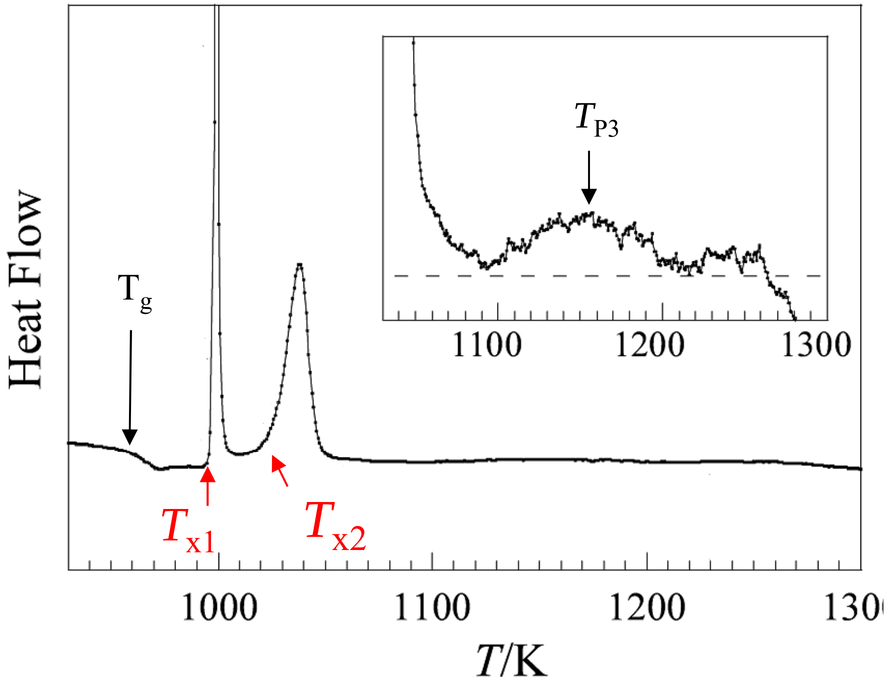

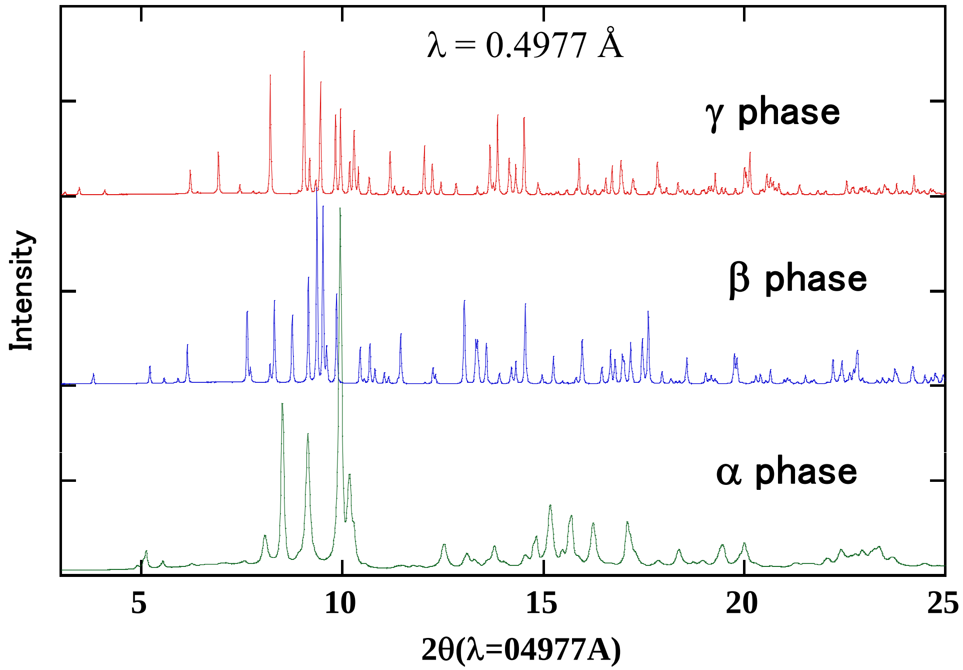

Before crystallization at 1150 K of the stable ferroelectric γ phase, two metastable phases α (at T_{x1}) and β (at T_{x2}) appeared in sequence.

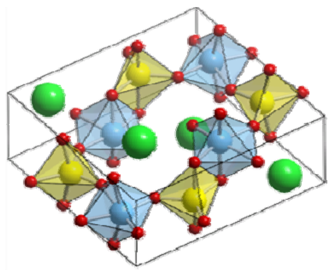

Paraelectric β phase

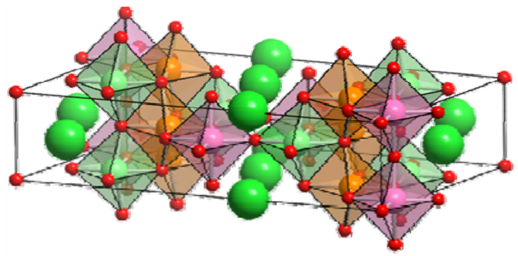

Ferroelectric γ phase

J.Yu *et al.*, Chem. Mater. **21**, (2009) 259.

Giant dielectric response at T_{x1}

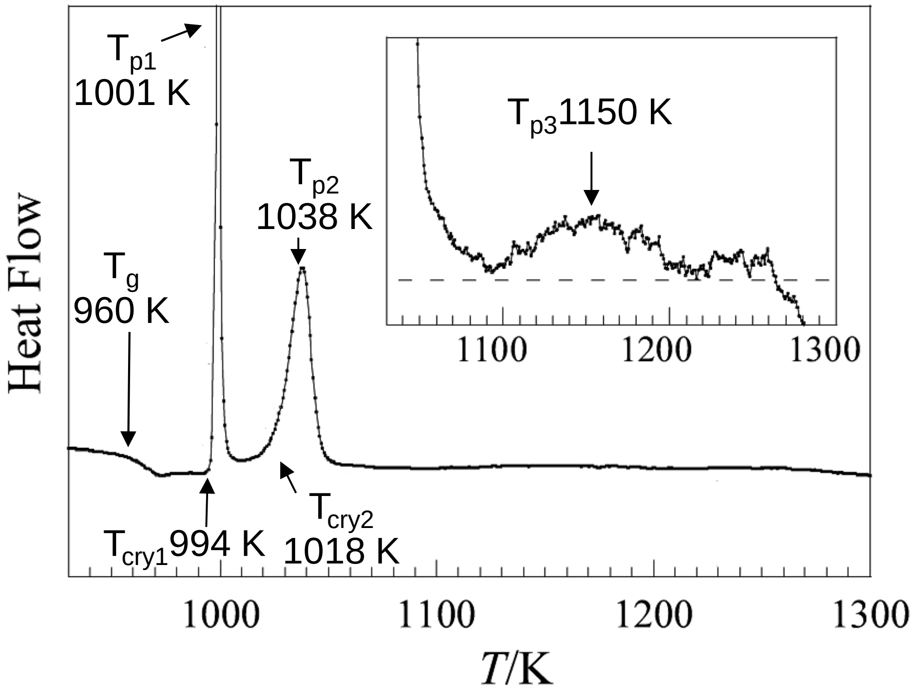

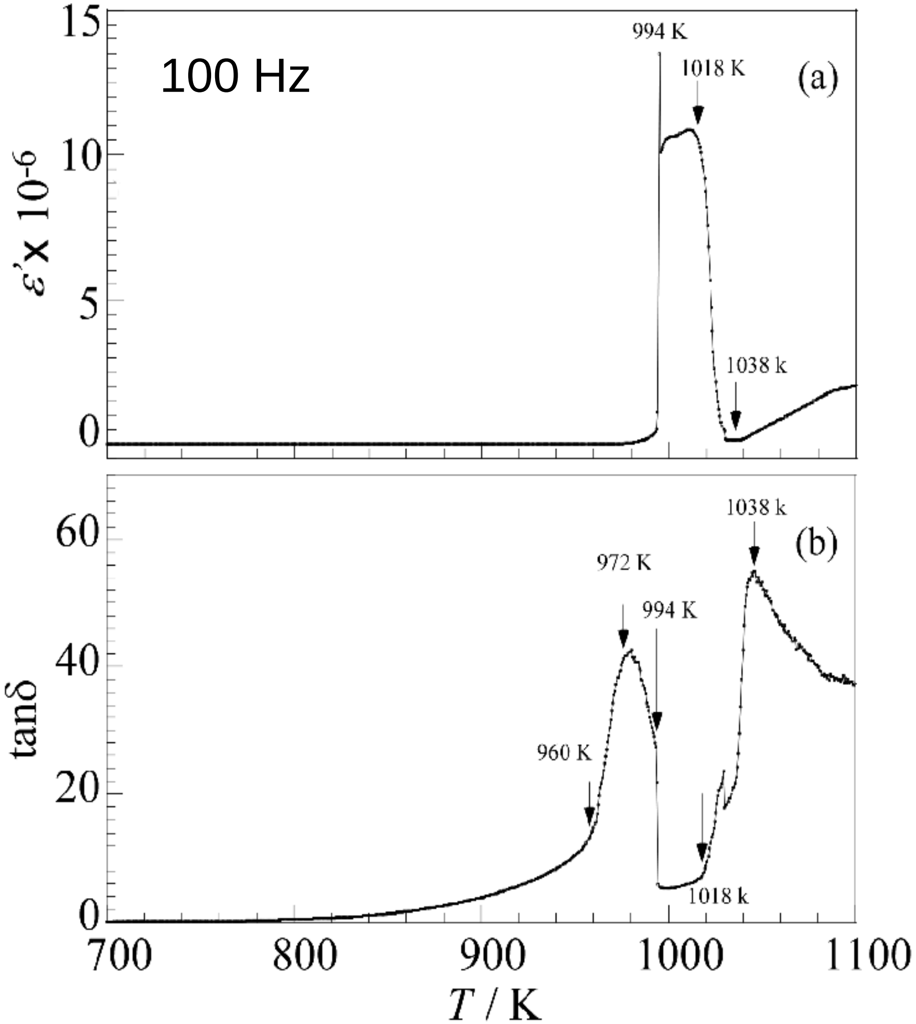

Measurement of Second harmonic generation

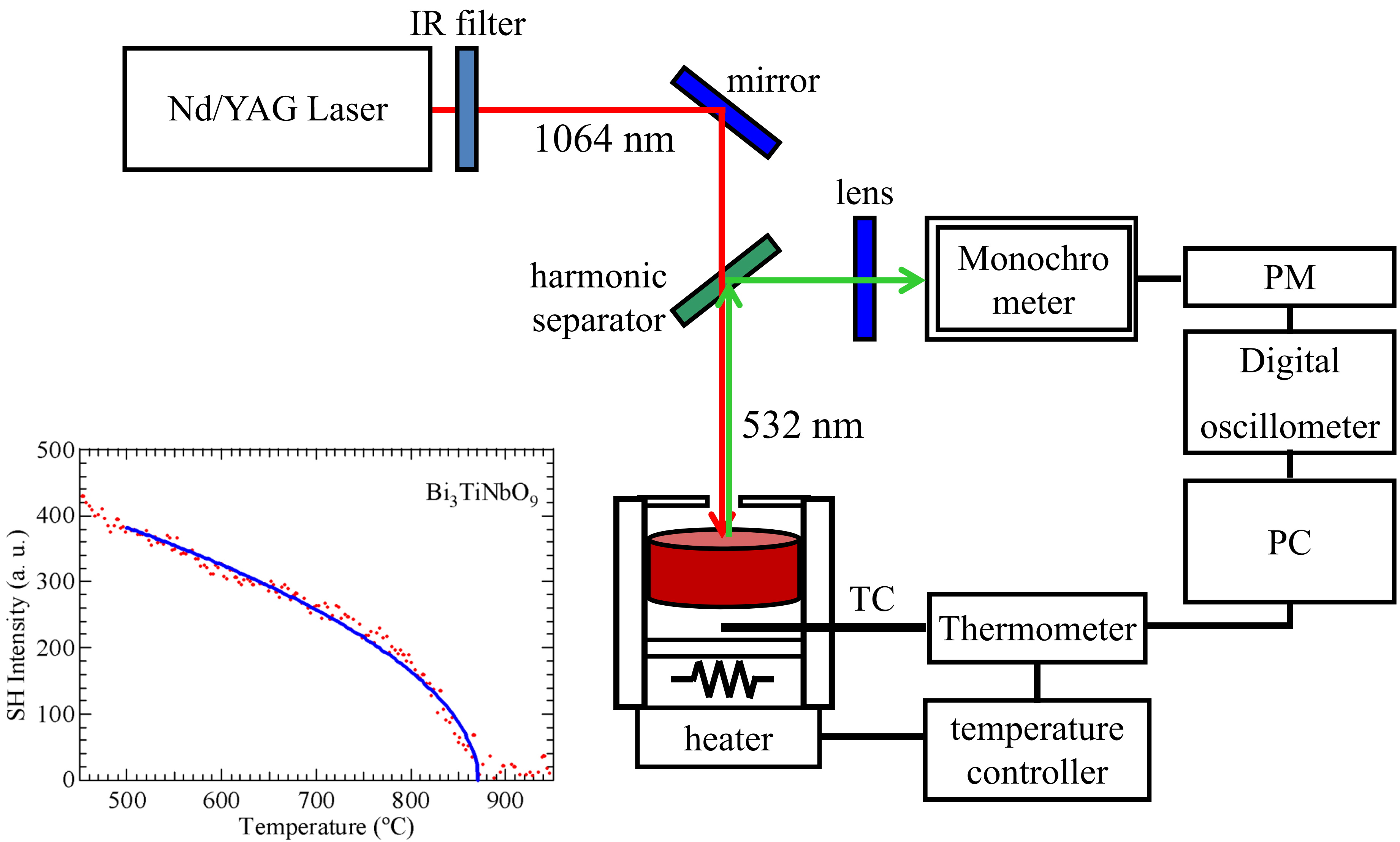

Giant Second harmonic generation at T_{x1}

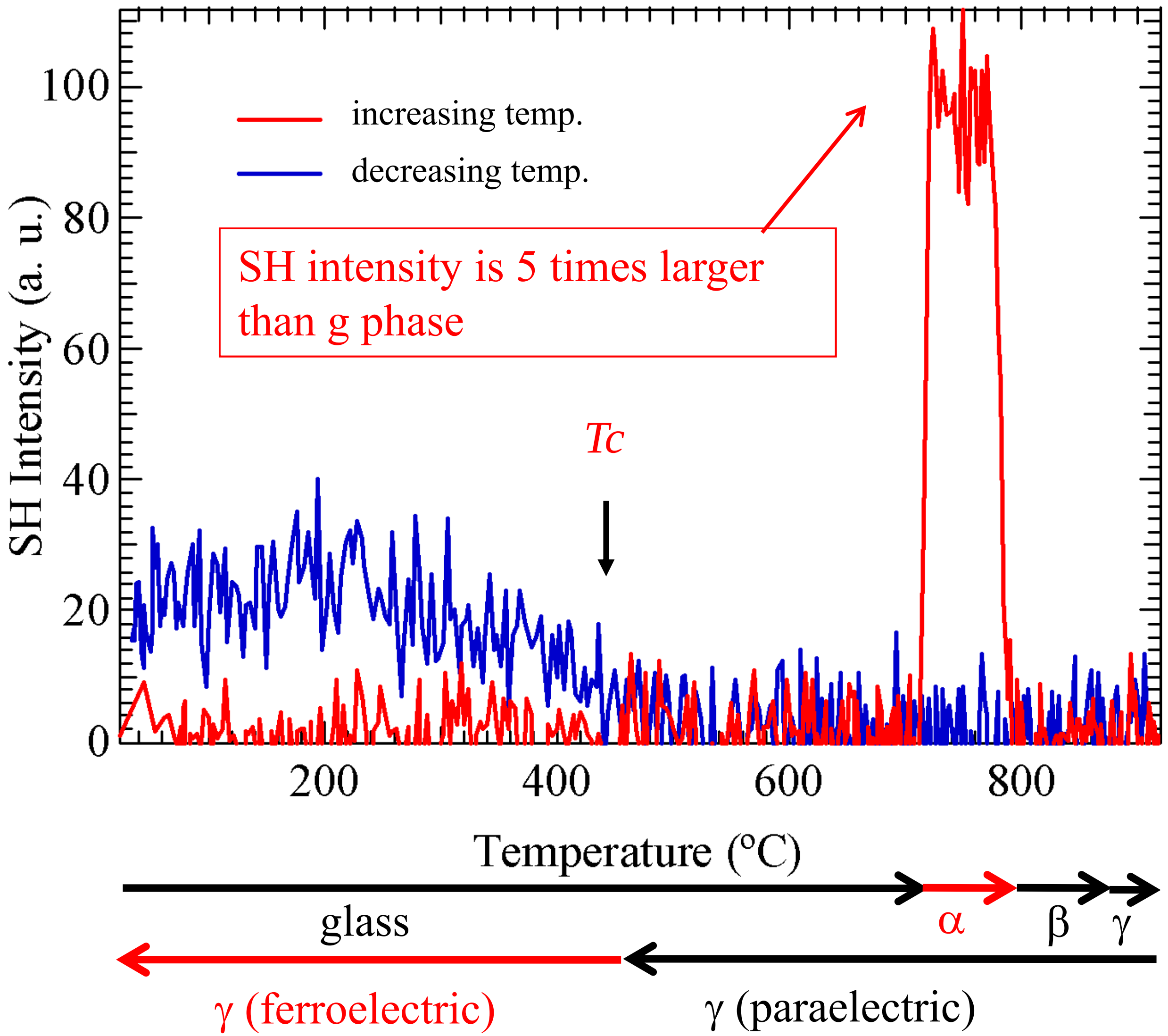

SHG appeared at T_{x1} and disappeared at T_{x2}.

This behavior totally corresponds to that of dielectric constant.

Direct evidence of correlation between α phase crystal structure and giant dielectric response

A. Masuno et al., Appl. Phys. Express **4**, (2011) 042601.

Mechanism of giant response at T_{x1}

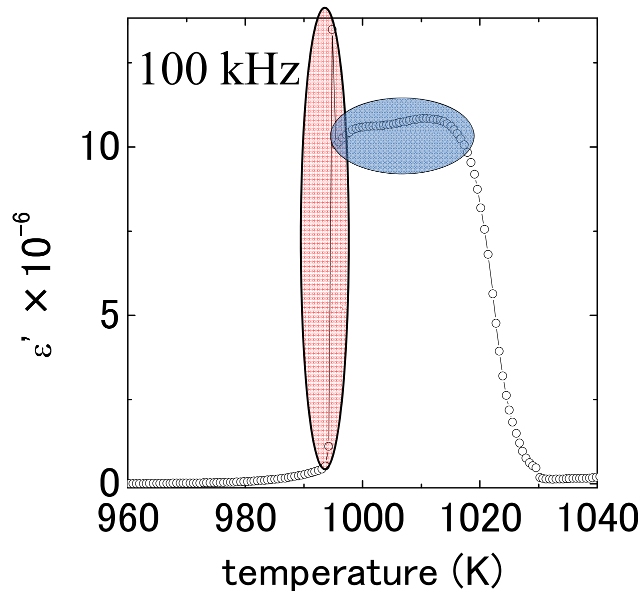

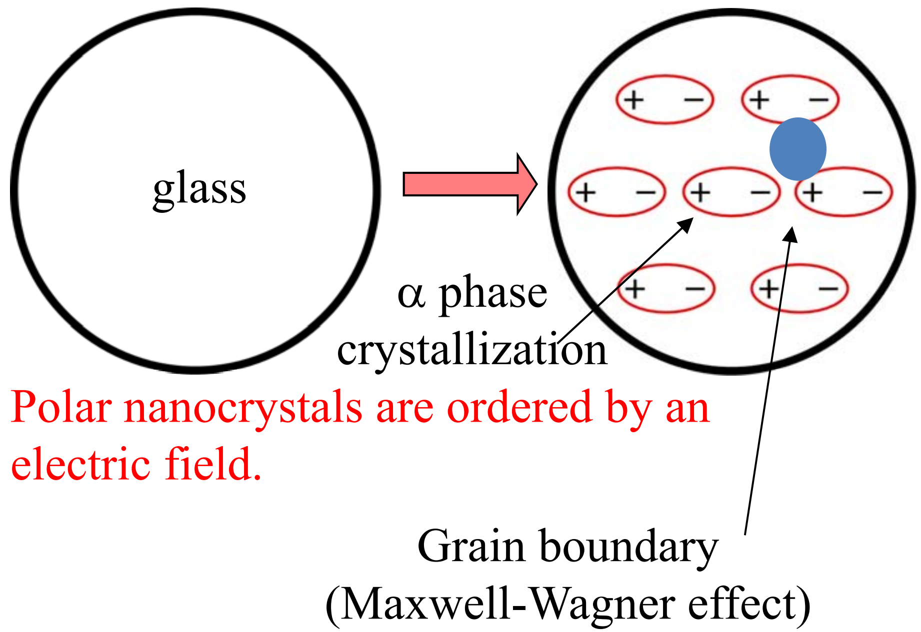

✓Giant SHG response at T_{x1}: α-$BaTi_2O_5$ has non-centrosymmetric (polar) structure.

✓The instant dielectric jump at T_{x1} was caused by the alignment of polar nanocrystals of α phase.

✓The large dielectric constant from T_{x1} to T_{x2} was explained by the Maxwell–Wagner effect at the grain boundaries between the glass and the partially crystallized α phase.

By *in-situ* SHG observation during crystallization process, we obtained the first direct evidence that the alignment of polar nanocrystals caused the giant dielectric response.

A. Masuno *et al.*, Appl. Phys. Express **4**, (2011) 042601.

$Ba_{1-x}Ca_xTi_2O_5$ glass

Crystallization of ferroelectric phase

Single phase crystallization from $BaTi_2O_5$ glass

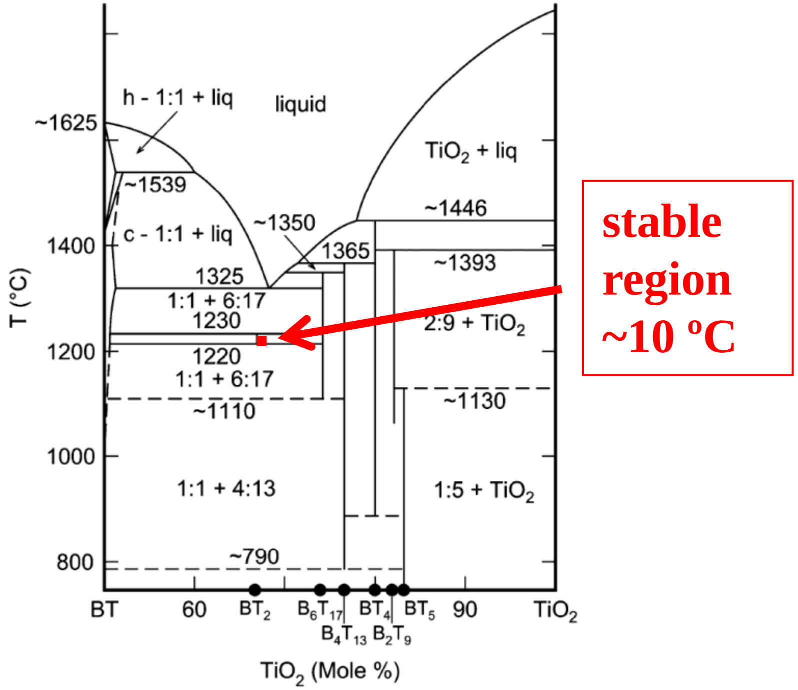

N. Zhu and A. R. West, J. Am. Ceram. Soc. **93**, (2010) 295.

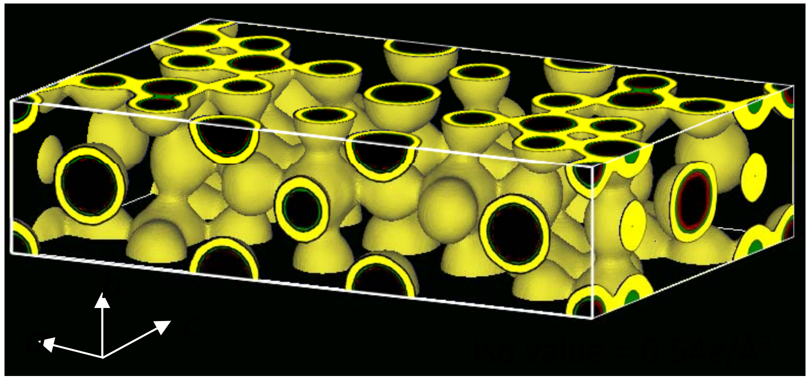

C. Moriyoshi *et al*., Jpn. J. Appl. Phys. **48**, (2009) 09KF06 .

We found that crystallization from the glass was useful for single phase preparation of $BaTi_2O_5$.

Control of ferroelectric properties by substitution for Ba as well as $BaTiO_3$ system.

Previous reports;

Sr : $Ba_{1-x}Sr_xTi_2O_5$ ($x < 0.12$)
→ arc-melt method

X. Yan *et al*., J. Ceram. Soc. Jpn. **115**, (2007) 648.

KF : $Ba_{1-x}K_xTi_2O_{5-x}F_x$ ($x < 0.05$)
→ sol-gel + SPS

J. Xu and Y. Akishige, Appl. Phys. Lett. **92**, (2008) 052902.

Results: heat treatment condition

$Ba_{1-x}Ca_xTi_2O_5$

	1000 ºC 10 min.	1000 ºC 12h.	1100 ºC 10 min.	1200 ºC 12 h.
0				○
0.05				○
0.07				○
0.10	○	○	○	×
0.12	○	△	○	
0.15	○	△		
0.20	○	△		
0.30	○	△		
0.40	×			

Heating rate: 20 ºC/min.
(5 ºC/min. for 1200 ºC)

○ : single phase
△ : slight impurity of $BaTiO_3$
× : almost no $BaTi_2O_5$ phase

$0 < x < 0.07$
as stable as $BaTi_2O_5$
$0.10 < x < 0.12$
decreasing stability
$0.15 < x < 0.30$
metastable phase
$0.40 < x$
no $Ba_{1-x}Ca_xTi_2O_5$ phase

Results: dielectric constant

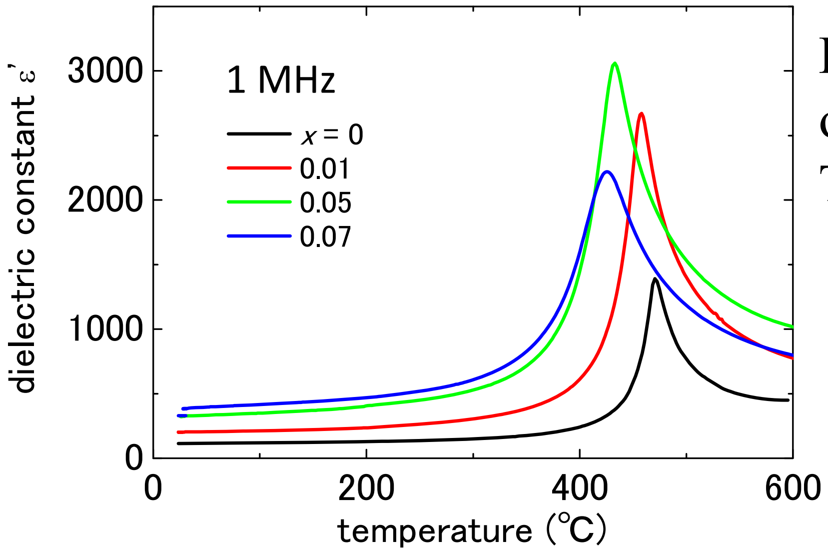

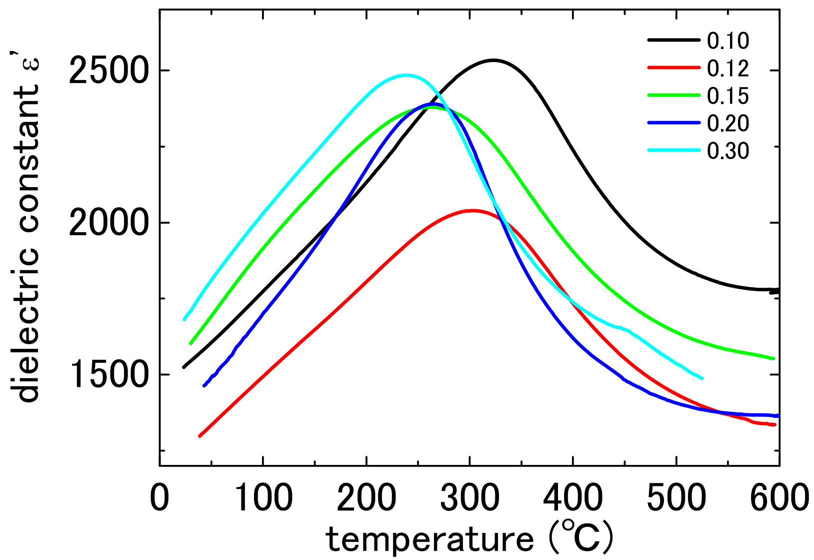

Ferroelectric transition temperatures were observed in all $Ba_{1-x}Ca_xTi_2O_5$ phases ($x \leq 0.30$) The peaks were broaden with increase of *x*.

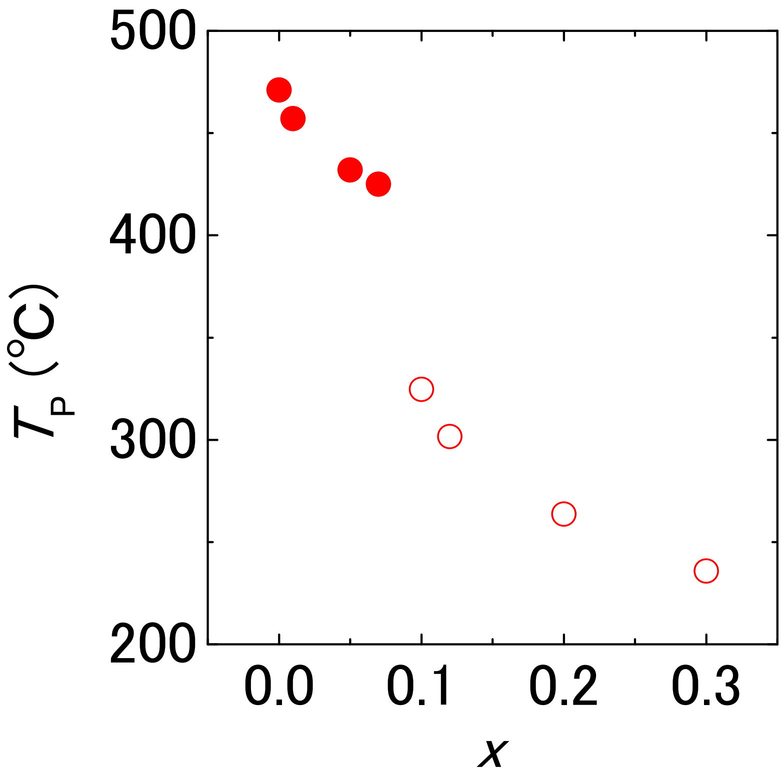

T_P dropped 250 °C.

Results: lattice constants

$Ba_{1-x}Ca_xTi_2O_5$

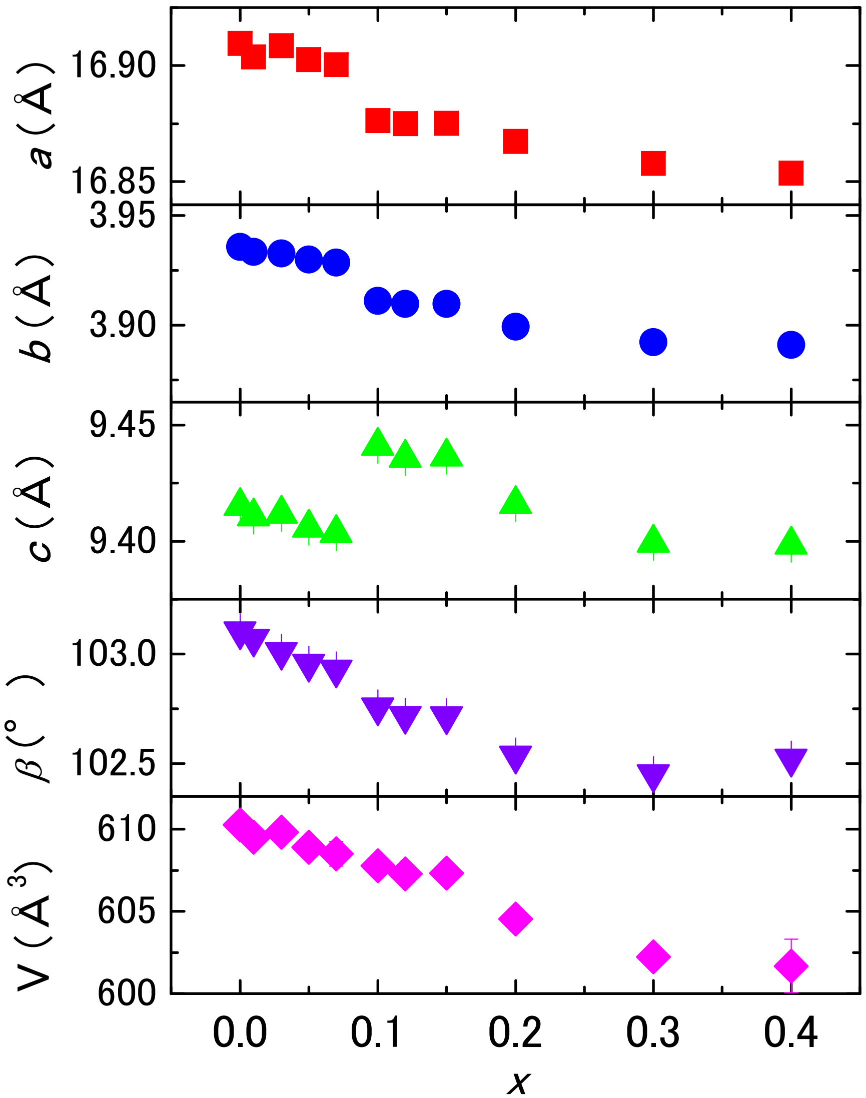

Change ratio of lattice constants

$$\Delta l / l_0 = (l_0 - l_x) / l_0$$

l_0: lattice constant at $x = 0$

l_x: lattice constant at x

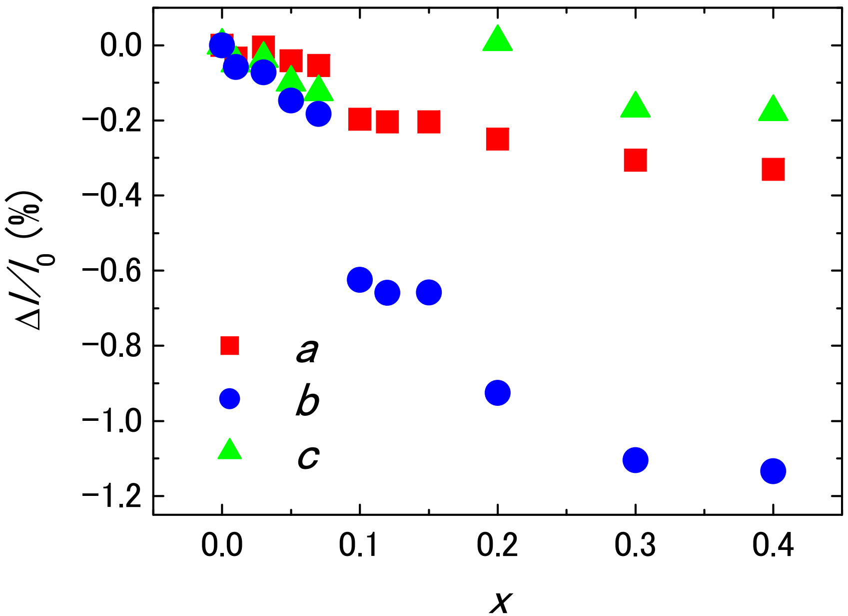

Decrease ratio of *b* axis is larger than other axes.

→affect ferroelectric properties effectively

Results: Correlation between T_P and *b* axis length

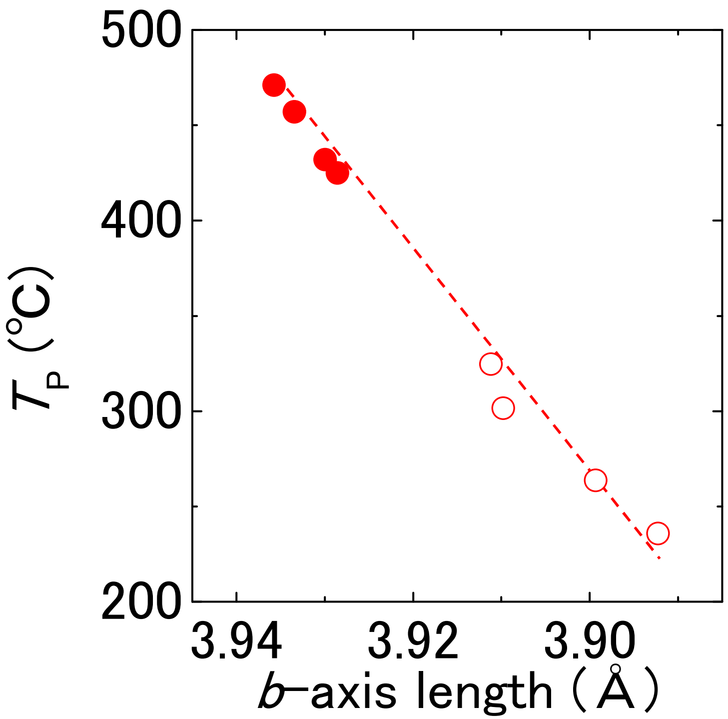

Strong correlation between T_P and *b* axis length

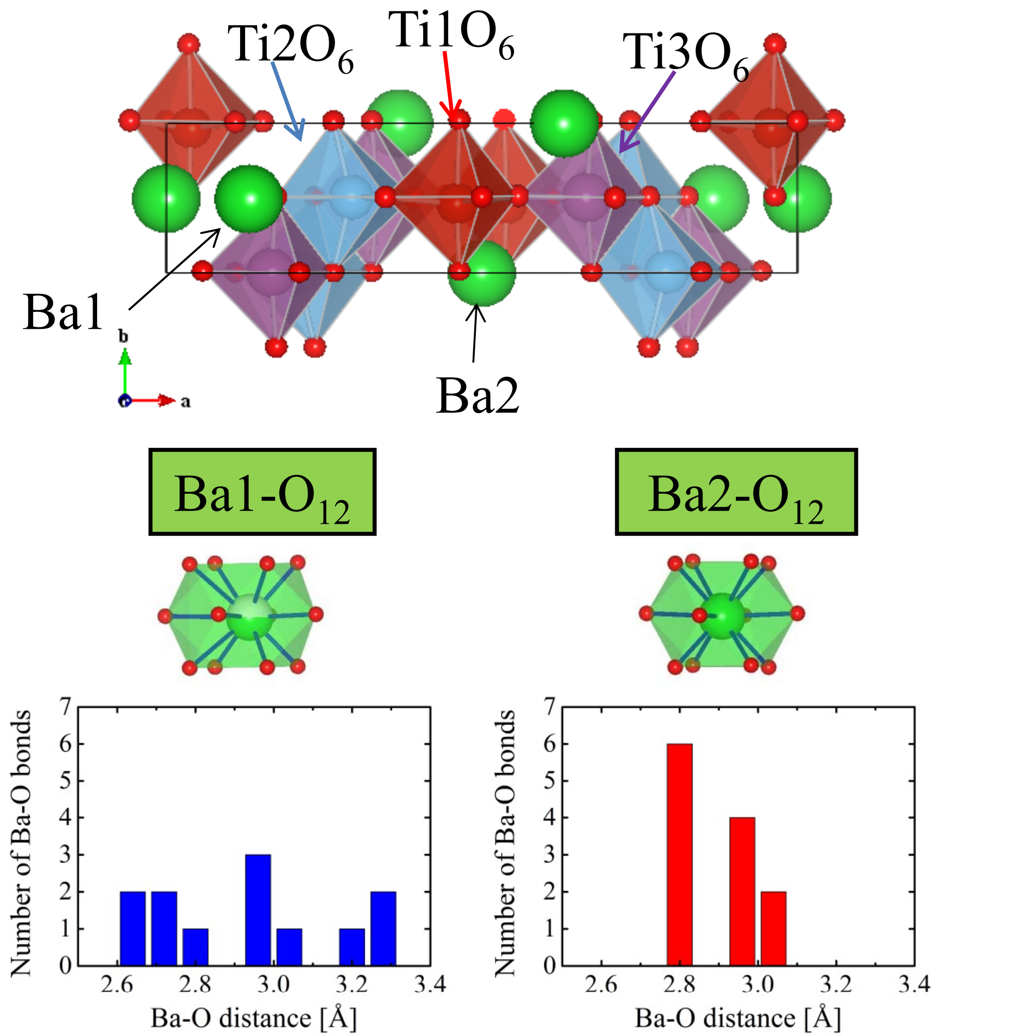

Ba-O bond length distribution in BaO_{12} polyhedra

Site selectivity of Ca in $Ba_{0.95}Ca_{0.05}Ti_2O_5$

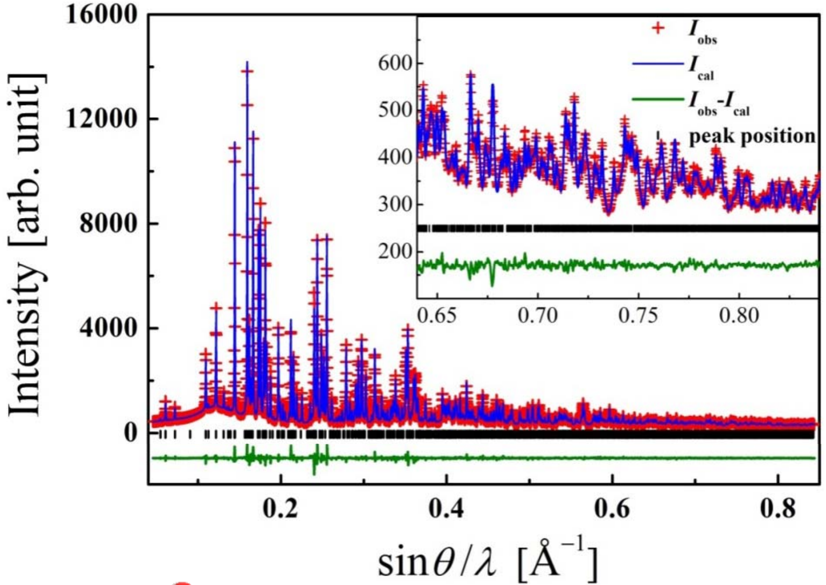

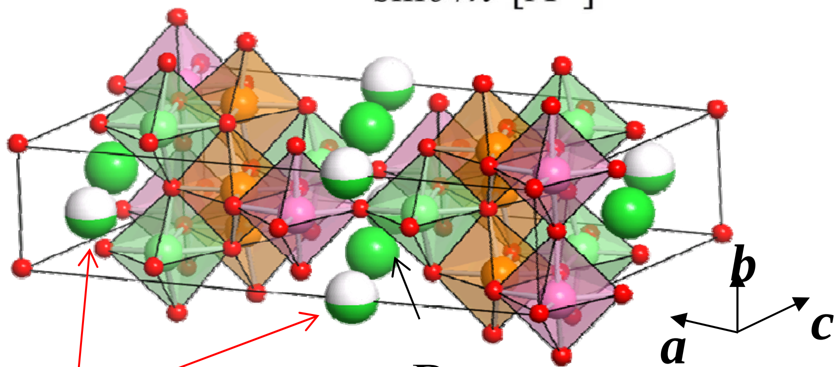

$Ba_{0.95}Ca_{0.05}Ti_2O_5$

Atom	*g*	*x*	*y*	*z*	*U* [10^{-2}Å^2]
Ba1	0.944(1)	0.36858(3)	-0.002(1)	0.01753(6)	0.647(7)
Ca1	0.056(1)	0.36858(3)	-0.002(1)	0.01753(6)	0.647(7)
Ba2	1	0	0.5	0.5	0.67(2)
Ti1	1	0.0390(1)	-0.024(1)	0.2096(2)	0.83(6)
Ti2	1	0.2073(1)	0.003(3)	0.3724(2)	0.70(4)
Ti3	1	0.3337(1)	0.504(3)	0.3044(2)	0.77(5)
O1	1	0.0356(3)	0.529(3)	0.2102(5)	0.3(2)
O2	1	0.1108(3)	0.028(3)	0.4271(5)	0.2(2)
O3	1	0.1510(3)	0.025(4)	0.1836(5)	0.2(2)
O4	1	0.1749(3)	0.510(8)	0.6608(5)	0.2(2)
O5	1	0.2344(3)	0.518(5)	0.3953(5)	0.2(2)
O6	1	0.2892(3)	0.518(6)	0.1249(6)	0.6(2)
O7	1	0.4424(3)	0.508(8)	0.2884(5)	0.3(2)
O8	1	0	0.01545	0	0.3(2)

C2, a = 16.9036(1) Å, b = 3.93030(2) Å, c = 9.40715(6) Å, β = 102.9640(4)°.

R_{WP} = 0.0290, R_I = 0.0173, R_F = 0.0104.

Ca ions occupy only the distorted Ba1 site.

C. Moriyoshi *et al.*, J. Phys. Soc. Jpn. **81**, (2011) 014706.

XANES spectra of Ca in $Ba_{1-x}Ca_xTi_2O_5$

$Ba_{1-x}Ca_xTi_2O_5$

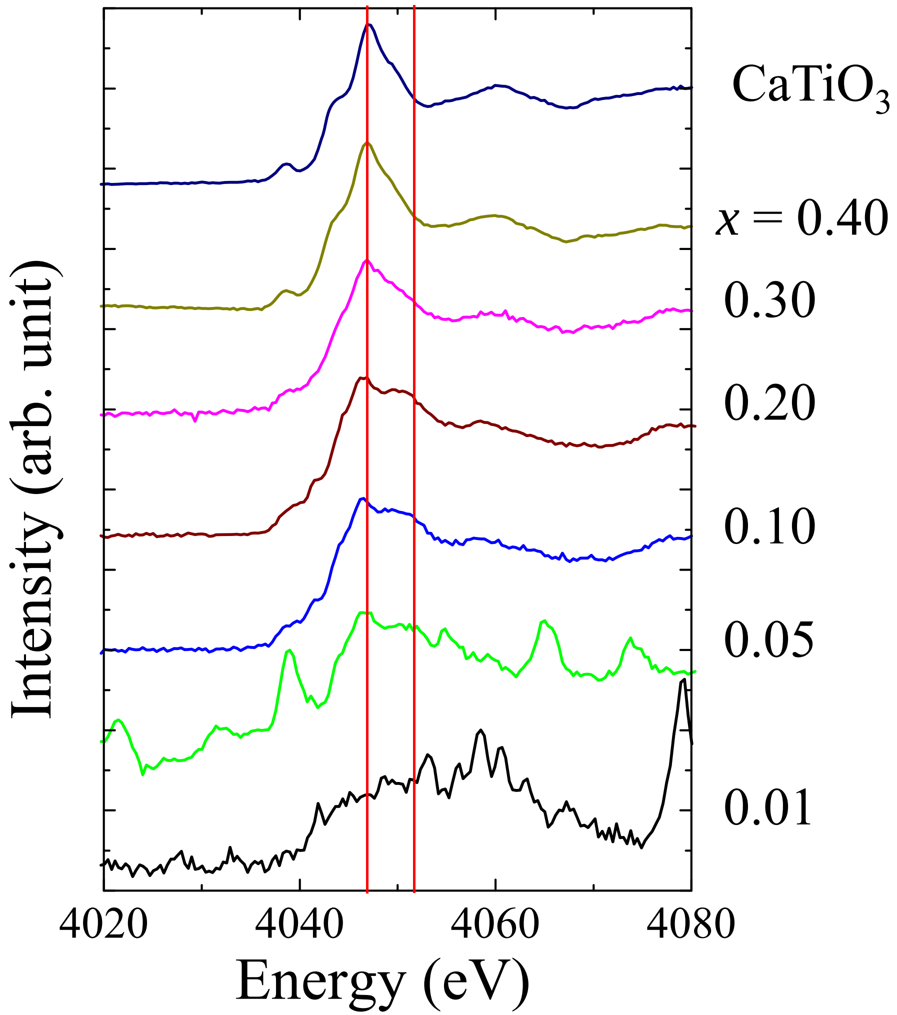

Fluorescence method at SAGA-LS

calculation

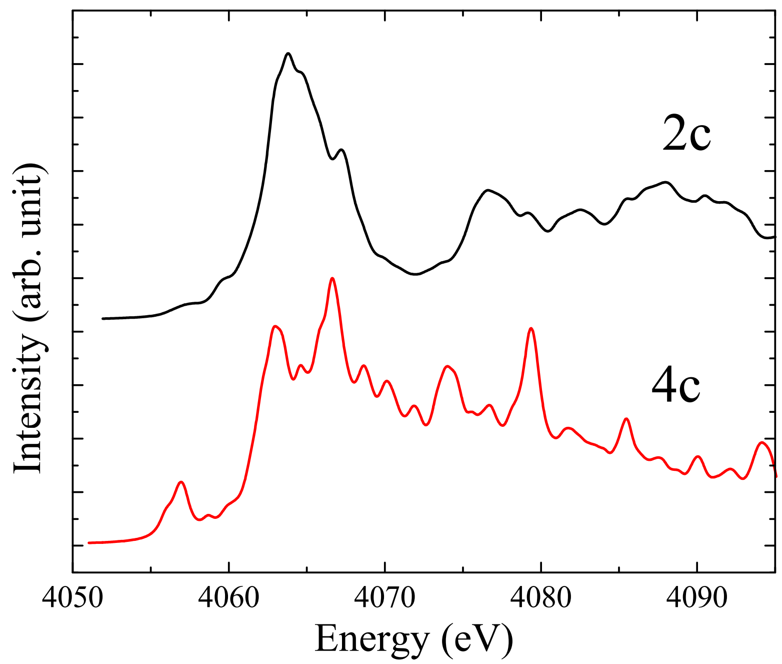

Ca site selectivity is realized only at low Ca concentration.
In metastable ferroelectric phase, Ca occupies both 2c and 4c sites.

Crystallization of ferroelectric phase

Ferroelectric phase crystallized from $Ba_{1-x}Ca_xTi_2O_5$ glass.

Ferroelectric properties depend on b-axis bond length.

$0 \leq x \leq 0.07$: stable phase
site selective Ca doping

$0.10 \leq x \leq 0.30$: metastable phase
random site doping of Ca

$Ba_{1-x}Ca_xTi_2O_5$ glass is useful as a precursor of ferroelectric phase.

Summary: TiO_2 glass system

✓Optical properties

Colorless and transparent in visible and near IR region

High refractive index > 2.1 and low wavelength dispersion

Strong upconversion luminescence due to low phonon energy

✓Glass forming region

binary (La_2O_3-TiO_2) and ternary (BaO-TiO_2-MO_x, La_2O_3-TiO_2-MO_x) systems were determined.

Ca doping caused characteristic changes in physical and structural properties.

✓Unusual crystallization process

Giant SHG response at a phase crystallization temperature.

Metastable ferroelectric phase crystallized from Ca doped glasses.

Nb_2O_5 system

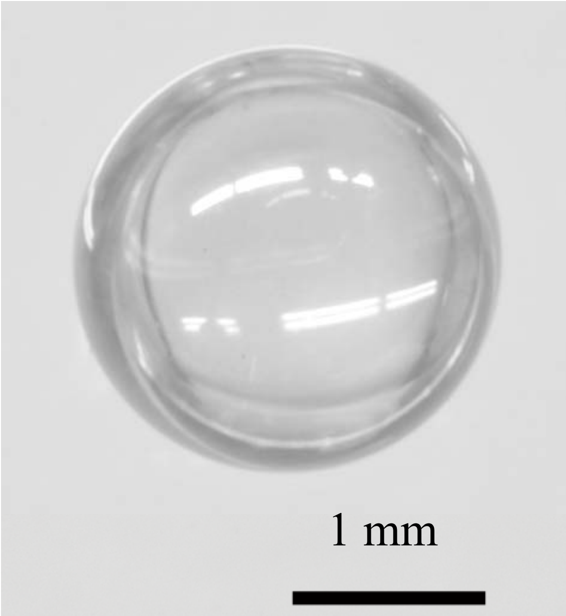

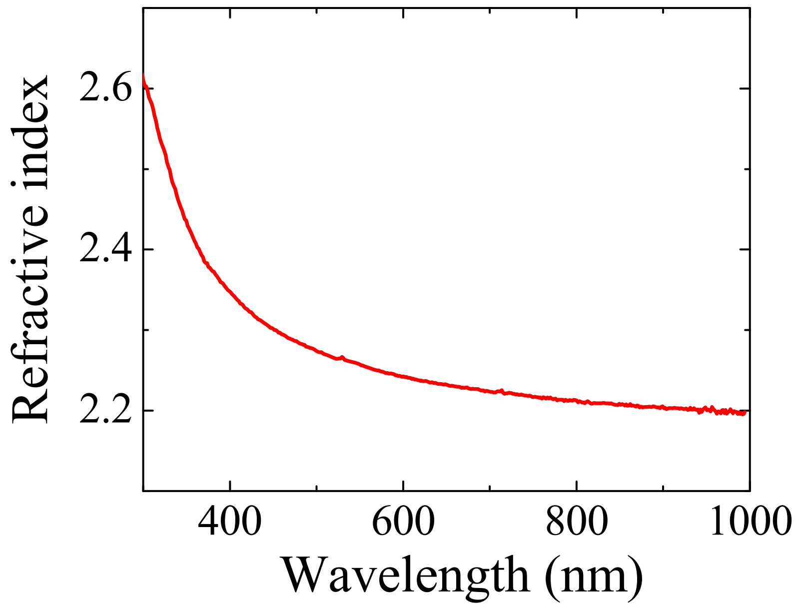

$0.30La_2O_3$-$0.70Nb_2O_5$
spherical glass was prepared
by containerless processing.
$\phi = 2 \sim 3$ mm

Colorless and transparent
High refractive index over 2.2

suitable for small optics used
in visible and infrared region

e.g. lens, endoscope, fiber collimator

A. Masuno and H. Inoue,
Appl. Phys. Express **3**, 10261 (2010).

New glass system ~ frontier in glass science ~

TiO_2, Nb_2O_5 glasses prepared by containerless processing

✓Without networkformer
✓Large oxygen packing density
✓Large oxygen polarizability

<u>Deviation from the classic glass forming rules</u>

Through investigating physical and structural properties,
new and extended glass forming rules should be made.

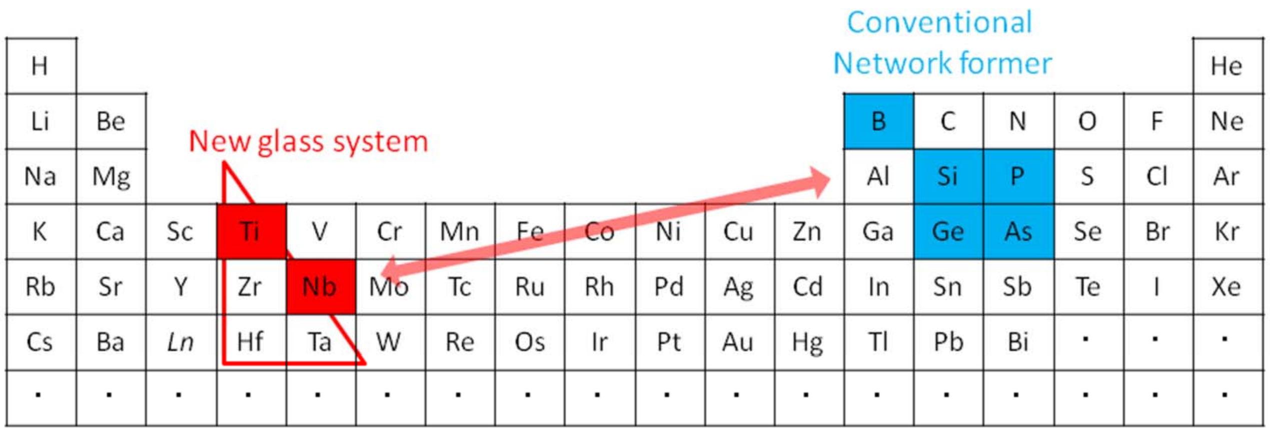

Refferences

1. Glass Formation in LaO3/2–TiO2 Binary System by Containerless Processing
   M. Kaneko, J. Yu, **A. Masuno**, H. Inoue, M. S. V. Kumar, O. Odawara, S. Yoda
   J. Am. Ceram. Soc. **95** (2012) 79.
2. Site-selective Calcium Substitution in BaTi2O5: Effect on the Crystal Structure and the Ferroelectric Phase Transition
   C. Moriyoshi, Y. Kuroiwa, **A. Masuno**, H. Inoue
   J. Phys. Soc. Jpn. **81**, (2011) 014706.
3. Structural-relaxation-induced high refractive indices of $Ba_{1-x}Ca_xTi_2O_5$ glasses
   A. Masuno, H. Inoue, Y. Arai, J. Yu, Y. Watanabe
   J. Mater. Chem. **21**, (2011) 17441.
4. Effect of substituting Al_2O_3 and ZrO_2 on thermal and optical properties of high refractive index La_2O_3-TiO_2 glass system prepared by containerless processing
   H. Inoue, Y. Watanabe, **A. Masuno**, M. Kaneko, J. Yu
   Opt. Mater. **33**, (2011) 1853.
5. Giant second harmonic generation from metastable $BaTi_2O_5$
   A. Masuno, Y. Kikuchi, H. Inoue, J. Yu, Y. Arai
   Appl. Phys. Express **4**, (2011) 042601.
6. Structure of Glassy and Metastable Crystalline BaTi2O5 Fabricated using Containerless Processing
   J. Yu, S. Yoda, **A. Masuno**, H. Natsui, M. Kaneko
   Ferroelectrics **402**, (2010) 130.
7. High Refractive Index of $0.30La_2O_3$-$0.70Nb_2O_5$ Glass Prepared by Containerless Processing
   A. Masuno and H. Inoue
   Appl. Phys. Express **3**, (2010) 102601.
8. Refractive index dispersion, optical transmittance, and Raman scattering of $BaTi_2O_5$ glass
   A. Masuno, H. inoue, J. Yu, Y. Arai
   J. Appl. Phys. **108**, (2010) 063520.
9. Charge Density Study of Metastable State in $BaTi_2O_5$ with Fivefold Coordinated Ti
   C. Moriyoshi, S. Miyoshi, Y. Kuroiwa, J. Yu, Y. Arai, **A. Masuno**
   Jpn. J. Appl. Phys. **49**, (2010) 09ME10.
10. Charge Density Study on Phase Transition in $BaTi_2O_5$ Ferroelectric
    C. Moriyoshi, N. Okizaki, Y. Kuroiwa, J. Yu, Y. Arai, **A. Masuno**
    Jpn. J. Appl. Phys. **48**, (2009) 09KF06
11. Comprehensive Structural Study of Glassy and Metastable Crystalline $BaTi_2O_5$
    J. Yu, S. Kohara, K. Itoh, S. Nozawa, S. Miyoshi, Y. Arai, **A. Masuno**, H. Taniguchi, M. Itoh, M. Takata, T. Fukunaga, S. Koshihara, Y. Kuroiwa, S. Yoda
    Chemistry of Materials **21**, (2009) 259.
12. Thermal stability and optical properties of Er^{3+} doped $BaTi_2O_5$ glasses
    A. Masuno, H. Inoue, J. Yu, Y. Arai, F. Otsubo
    Adv. Mater. Res. **39-40** (2008) 243.